1 **Serotonin signals through postsynaptic Gα_q, Trio RhoGEF, and DAG to promote**

2 ***C. elegans* egg-laying circuit activity and behavior**

3 Pravat Dhakal, Sana Chaudhry, and Kevin M. Collins*

4 Department of Biology, University of Miami, Coral Gables, FL, United States of America

5 *To whom correspondence should be addressed. Email: *kevin.collins@miami.edu*

6 *60 pages with 6 Figures, 2 Tables and 3 Movies*

Abstract

Activated $G\alpha_q$ signals through Phospholipase-Cβ (PLCβ) and Trio, a Rho GTPase exchange factor (RhoGEF), but how these distinct effector pathways promote cellular responses to neurotransmitters like serotonin remains poorly understood. We used the egg-laying behavior circuit of *C. elegans* to determine whether PLCβ and Trio mediate serotonin and $G\alpha_q$ signaling through independent or related biochemical pathways. Using genetic rescue experiments, we find that PLCβ functions in neurons while Trio RhoGEF functions in both neurons and the postsynaptic vulval muscles. While $G\alpha_q$, PLCβ, and Trio RhoGEF mutants all fail to lay eggs in response to serotonin, optogenetic stimulation of the serotonin releasing HSN command neurons restores egg laying only in PLCβ mutants. PLCβ mutants showed vulval muscle Ca^{2+} transients while strong $G\alpha_q$ and Trio RhoGEF mutants had little or no vulval muscle Ca^{2+} activity. Treatment with Phorbol esters that mimic Diacylglycerol (DAG), a product of PIP_2 hydrolysis, rescued egg-laying circuit activity and behavior defects of $G\alpha_q$ signaling mutants, suggesting both Phospholipase C and Rho signaling promote synaptic transmission and egg-laying via DAG production. DAG activates effectors including UNC-13, however, we find that phorbol esters, but not serotonin, stimulate egg laying in *unc-13* and PLCβ mutants. These results support a model where serotonin signaling through $G\alpha_q$, PLCβ, and UNC-13 promote neurotransmitter release, and that serotonin also signals through $G\alpha_q$, Trio RhoGEF, and an unidentified PMA-responsive effector to promote postsynaptic muscle excitability. Thus, the same neuromodulator serotonin can signal in distinct cells and effector pathways to coordinate activation of a motor behavior circuit.

Introduction

Neurons communicate in circuits via synaptic transmission to initiate, sustain, and terminate behaviors. During neurotransmission, both synaptic vesicles and dense-core vesicles fuse with the presynaptic membrane, releasing neurotransmitters and neuropeptides that activate postsynaptic ion channels and G protein coupled receptors (GPCRs) (Betke et al., 2012; Geppetti et al., 2015). While much has been learned about neurotransmitter signaling pathways through ionotropic receptors, the diversity of GPCRs and their signaling pathways has complicated our understanding of how their signaling exerts changes on cell excitability and behavior. The G protein, $G\alpha_q$, is one of the major G proteins expressed in all excitable cells (Offermanns, 2001; Simon et al., 1991; Wilkie et al., 1992). Activated $G\alpha_q$ signals through PIP_2-specific phospholipase-Cβ (PLCβ) to generate the second messengers, inositol 1,4,5 trisphosphate (IP_3) and diacylglycerol (DAG). IP_3 activates the IP_3 receptor to release Ca^{2+} from intracellular stores and activate downstream kinases, lipases, and ion channels (Berridge et al., 2000; Huang, 1989; Li et al., 2014; Mujica and Gonzalez, 2011). The membrane lipid DAG has been shown to recruit and activate numerous effector proteins including UNC-13 and Protein Kinase C (Ananthanarayanan et al., 2003; Brose and Rosenmund, 2002; Lou et al., 2008; Maruyama and Brenner, 1991; Rozengurt et al., 1997; Silinsky and Searl, 2003; Thore et al., 2005), but whether these or other identified DAG targets function to transduce all forms of $G\alpha_q$ signaling *in vivo* remains an open question.

Genetic studies in the nematode worm *C. elegans* show that $G\alpha_q$ signaling through both PLCβ, and Trio promotes neurotransmitter and neuropeptide transmission. In *C. elegans unc-73* gene encodes at least 8 isoforms of Trio, which has both Rac and Rho GTPase exchange factor (GEF) DH/PH domains (Steven et al., 2005; Williams et al., 2007). *unc-73* mutations that specifically affect the second Rho activating DH/PH GEF domain of Trio (Trio RhoGEF) disrupt locomotion, feeding, and egg-laying behaviors (Williams et al., 2007), without causing the axon

53 pathfinding and neurodevelopmental defects observed in animals bearing *unc-73* Trio RacGEF
54 mutations that affect the first, Rac activating DH/PH GEF domain (Steven et al., 1998). In worms,
55 $G\alpha_q$ knockouts are lethal while PLCβ or Trio RhoGEF single knockouts show defects in
56 neurotransmission that disrupt locomotion, feeding, egg-laying and other behaviors, resembling
57 $G\alpha_q$ loss-of-function mutants (Bastiani et al., 2003; Brundage et al., 1996; Hajdu-Cronin et al.,
58 1999; Lackner et al., 1999). Worms bearing mutations that disrupt both PLCβ and Trio RhoGEF
59 phenocopy the larval arrest phenotype of $G\alpha_q$ null mutants, consistent with these two effectors
60 relaying most or all of the relevant $G\alpha_q$ signaling (Williams et al., 2007). Genetic and biochemical
61 studies showed that $G\alpha_q$ binding to and activation of the Trio RhoGEF domain to promote Rho
62 signaling is conserved in mammals (Chhatriwala et al., 2007; Rojas et al., 2007), however, it
63 remains unclear how PLCβ and Rho signaling promotes neurotransmitter and neuropeptide
64 release *in vivo*. The larval lethality of $G\alpha_q$ null mutants can be rescued by the DAG-mimetic
65 phorbol ester, PMA (Reynolds et al., 2005), and PMA can also rescue the egg-laying defects of
66 PLCβ, Trio RhoGEF double mutants (Williams et al., 2007). These results suggest $G\alpha_q$ signaling
67 through both PLCβ and Trio may ultimately converge to regulate DAG levels and the activation
68 of downstream effectors. Both PLCβ and Trio RhoGEF promote acetylcholine (ACh) release
69 from motor neurons that control locomotion (Lackner et al., 1999; Miller et al., 1999; Williams et
70 al., 2007), although mutations in Trio RhoGEF cause behavior defects more aligned with a
71 function in dense core vesicle release (Hu et al., 2011). PLCβ is expressed in the nervous system
72 and intestine (Lackner et al., 1999), while $G\alpha_q$ and Trio show additional postsynaptic expression
73 in muscles (Bastiani et al., 2003; Lackner et al., 1999; Steven et al., 1998; Steven et al., 2005).
74 While re-expression of PLCβ in motor neurons (Lackner et al., 1999) or Trio in all neurons
75 (Williams et al., 2007) rescue the locomotion behavior defects of their mutants, prior work has
76 shown that $G\alpha_q$ has additional functions in muscles (Bastiani et al., 2003) to promote egg laying

77 where Trio RhoGEF is also expressed (Steven et al., 2005). Indeed, loss of PLCβ fails to
78 suppress the hyperactive egg-laying phenotypes of $G\alpha_q$ gain-of-function mutants, consistent
79 with $G\alpha_q$ signaling through other effectors like Trio RhoGEF to regulate egg laying (Bastiani et
80 al., 2003). Indeed, *unc-73* RhoGEF mutations strongly suppress the hyperactive egg-laying
81 behavior phenotypes of $G\alpha_o$ mutants unable to inhibit $G\alpha_q$ signaling (cite Williams et al. 2007).
82 Using genetics, optogenetics, pharmacology, and Ca^{2+} imaging techniques we have
83 investigated how $G\alpha_q$ and its two effector pathways regulate egg-laying circuit activity and
84 behavior. We find that PLCβ functions in the presynaptic neurons while Trio RhoGEF signals in
85 both neurons and muscles to promote egg laying. Loss of each of these effectors imparts specific
86 defects in egg-laying behavior that indicate these proteins function in distinct cells to promote
87 egg-laying circuit activity and behavior. Many of these defects can be rescued in part by
88 treatment with phorbol esters that mimic DAG production. These results clarify that despite $G\alpha_q$
89 signaling through independent PLCβ and Trio RhoGEF pathways, these effectors may ultimately
90 converge to potentiate DAG levels which promote egg-laying behavior.

91 **MATERIALS AND METHODS**

92 **Strains**

93 *C. elegans* worms were maintained at 20°C on Nematode Growth Medium (NGM) agar plates
94 with *E. coli* OP50 as a source of food as described previously (Brenner, 1974). All behavior
95 assays and fluorescence imaging experiments were performed with age-matched adult
96 hermaphrodites aged 24-36 h after the late L4 stage. All strains used in this study are listed in
97 Table 1.

98

99 **Molecular biology and transgenes**

100 **Vulval muscle GCaMP5 strains**

101 Vulval muscle Ca^{2+} activity was recorded using GCaMP5G (Akerboom et al., 2013) which was
102 expressed along with mCherry from the *unc-103e* promoter (Collins and Koelle, 2013), as
103 previously described (Collins et al., 2016; Ravi et al., 2018a). The wild-type reporter strain,
104 LX1918 *vsIs164 [unc-103e::GCaMP5::unc-54 3'UTR + unc-103e::mCherry::unc-54 3'UTR + lin-*
105 *15(+)] lite-1(ce314) lin-15(n765ts) X* was used as described previously (Collins et al., 2016).
106 LX1918 males were crossed separately into DA823 *egl-30(ad805) I*, MT1434 *egl-30(n686) I*,
107 JT47 *egl-8(sa47) V*, MT1083 *egl-8(n488) V*, KG1278 *unc-73(ce362) I*, LX1226 *eat-16(tm761) I*,
108 CG21 *egl-30(tg26) I*, *him-5(e1490) V*, or KP1097 *dgk-1(nu62) X* hermaphrodites to generate
109 MIA140 *egl-30(ad805) I; vsIs164 lite-1(ce314) lin-15(n765ts) X*, MIA139 *egl-30(n686) I; vsIs164*
110 *lite-1(ce314) lin-15(n765ts) X*, MIA109 *egl-8(sa47) V; vsIs164 lite-1(ce314) lin-15(n765ts) X*,
111 MIA288 *egl-8(n488) V; vsIs164 lite-1(ce314) lin-15(n765ts) X*, MIA141 *unc-73(ce362) I; vsIs164*
112 *lite-1(ce314) lin-15(n765ts) X,* MIA287 *eat-16(tm761) I; vsIs164 lite-1(ce314) lin-15(n765ts) X*,
113 MIA286 *egl-30(tg26) I; vsIs164 lite-1(ce314) lin-15(n765ts) X* ,and MIA296 *dgk-1(nu62) vsIs164*
114 *lite-1(ce314) lin-15(n765ts) X*, respectively. The corresponding gene mutation was confirmed by
115 phenotype, genotype, or both. Presence of *vsIs164* was confirmed observing the mCherry

116 marker, and *lite-1(ce314) X* was confirmed with PCR genotyping. Oligo sequences used for
117 genotyping the corresponding mutations are shown in Table 2.
118
119 **Trio RhoGEF-E transgenes**
120 *Pan-neuronal expression*:
121 The *rab-3* promoter was used to drive expression of GFP alone or with Trio-RhoGEF-E. Briefly,
122 plasmids KG#68 (*rab-3p::GFP*; 15 ng/µl) alone or with KG#281 (*rab-3p:: unc-73e;* 50 ng/µL)
123 were injected into KG1278 *unc-73(ce362) I* (Williams et al., 2007). For behavior experiments,
124 five independent GFP-expressing transgenic lines were used, from which a single transgenic
125 line from each was kept: MIA374 *unc-73(ce362) I*; *keyEx66* (expressing GFP alone) and MIA375
126 *unc-73(ce362) I*; *keyEx67* (expressing GFP and Trio RhoGEF-E). Plasmids KG#281(*rab-*
127 *3p::unc-73e*) and KG#68(*rab-3p::GFP*) were kind gifts from Dr. Kenneth Miller.
128
129 *Pan-muscle expression*
130 Plasmid pKMC33 (*rgs-1p::mCherry*) was digested with NheI/KpnI and ligated with similarly
131 digested pPD96.52 (Fire lab *C. elegans* Vector Kit 1999; 1608: L2534, Addgene) to generate
132 pKMC166 (*myo-3p::mCherry*). Plasmid KG#281 (*rab-3p::unc-73e*) was digested with NheI and
133 KpnI, and the insert was ligated into similarly digested pKMC166 to generate pPD3 (*myo-*
134 *3p::unc-73e*). pKMC166 (15 ng/µL) alone or with pPD3 (50 ng/µL) was injected into KG1278
135 *unc-73(ce362) I* mutants. Five independent mCherry-expressing transgenic lines were used for
136 behavior experiments from which a single transgenic line from each was kept: MIA376 *unc-*
137 *73(ce362) I; keyEx68* (expressing mCherry alone) and MIA377 *unc-73(ce362) I*; *keyEx69*
138 (expressing mCherry + Trio RhoGEF-E).
139
140 Neuron and muscle co-expression

141 Plasmids KG#68 (15 ng/µl; pan-neuronal GFP) or pKMC166 (15 ng/µl; pan-muscle mCherry)
142 alone or with KG#281 (50ng/µl; pan-neuronal *unc-73e*) and pPD3 (50ng/µL; pan-muscle *unc-*
143 *73e*) were injected into KG1278 *unc-73(ce362) I*, generating five independent mCherry(+),
144 GFP(+) transgenic lines for behavior experiments from which a single transgenic line from each
145 was kept: MIA372 *unc-73(ce362); keyEx64* expressing mCherry (muscles) and GFP (neurons)
146 only and MIA373 *unc-73(ce362); keyEx65* expressing GFP (neurons), mCherry (muscles) and
147 TrioRhoGEF-E (both neurons and muscles).
148
149 **PLCβ Transgenes**
150 To generate a control plasmid expressing GFP in neurons, GFP coding sequences were
151 amplified from pJM60 (Moresco and Koelle, 2004) using oligonucleotides RE-GFP-FWD / -REV,
152 digested with NheI / KpnI, and ligated into similarly digested pGP3 bearing the *rgs-1* promoter
153 (Dong et al., 2000), generating pKMC78. An *egl-8* cDNA was used to generate and express a
154 functional GFP fusion protein in neurons. Briefly, oligonucleotides egl-8-cDNA-fwd / -rev were
155 used to amplified *egl-8* coding sequences from a plasmid bearing an *egl-8* cDNA provided by
156 Dr. Kenneth Miller (pKP309). This amplicon was digested with NheI / NcoI and ligated into a
157 similarly digested pPD49.26 plasmid, generating pKMC193. Quickchange mutagenesis with
158 oligonucleotides egl-8-Cterm-NotI-fwd / -rev were used to insert an in-frame NotI site near the 3'
159 end of the *egl-8* cDNA in a divergent region of the coding sequence, generating plasmid
160 pKMC194. Coding sequences for *egl-8* bearing this NotI site were then moved to pKMC78 by
161 digestion of pKMC194 with NheI/NcoI followed by ligation into a similarly digested pKMC78,
162 generating pKMC195. Oligonucleotides NotI-GFP-FWD / -REV were used to amplified GFP
163 coding sequences from pKMC78, digested with NotI, and ligated into a similarly digested
164 pKMC195, generating pKMC196. A strain bearing the *egl-8(sa47)* mutation was generously
165 provided by Dr. Joshua Kaplan and backcrossed four times to N2 wild-type animals to generate

166 LX1225 *egl-8(sa47) V.* MT8189 *lin-15(n765ts)* males were mated to LX1225 to generate LX1287
167 *egl-8(sa47) V; lin-15(n765ts) X* hermaphrodites that were kept at 15°C prior to injection.
168 Plasmids expressing GFP alone (pKMC78; 5 ng/µl) or *egl-8* CDNA fused to GFP (pKMC196; 5
169 ng/µl) were injected along with pL15EK (50 ng/µl) into LX1287 hermaphrodites. For behavior
170 experiments, five independent GFP-expressing lines were used from which a single transgenic
171 line (*vsEx679* [GFP] and *vsEx680* [EGL-8::GFP], respectively) was kept. We noted that
172 transgenic expression of GFP alone did cause a modest, but significant reduction of egg
173 accumulation compared to LX1225 *egl-8(sa47) V* mutant animals. This effect appeared to be
174 specific for egg accumulation, as these same *egl-8(sa47)* GFP-only expressing transgenic lines
175 showed similar resistance to 1 mM aldicarb as LX1225 *egl-8(sa47) V* (0 ±2.1% vs. 9 ±5.9% of
176 animals paralyzed at 4 h, respectively). In contrast, 48 ± 7.9% of transgenic *egl-8(sa47)* animals
177 expressing EGL-8::GFP were paralyzed at 4 h, not significantly different to wild-type N2 animals
178 (51 ±9.6% of animals paralyzed at 4 h).
179
180 **Vulval muscle Channelrhodopsin-2 strains**
181 N2 males were crossed into MIA229 *keyIs48 [ceh-24p::ChR2::unc-54 3'UTR + lin-15(+)], lite-*
182 *1(ce314), lin-15(n765ts) X* (Kopchock et al., 2021) to produce F1 heterozygous males, which
183 then were crossed separately into MIA211 *unc-73(ce362) I; lite-1(ce314) lin-15(n765ts) X,*
184 MIA299 *egl-30(ad805) I; lite-1(ce314) lin-15(n765ts) X*, MIA303 *egl-8(n488) V; lite-1(ce314) lin-*
185 *15(n765ts) X*, or MIA307 *egl-8(sa47) V; lite-1(ce314) lin-15(n765ts) X* hermaphrodites to
186 generate vulval muscle specific Channelrhodopsin-2 (ChR2) expressing transgenic lines
187 MIA248 *unc-73(ce362) I; keyIs48; lite-1(ce314) X*, MIA301 *egl-30(ad805) I; keyIs48; lite-*
188 *1(ce314) X*, MIA305 *egl-8(n488) V; keyIs48; lite-1(ce314) X*, and MIA309 *egl-8(sa47) V;*
189 *keyIs48; lite-1(ce314) X*. The presence of *lite-1(ce362)* was confirmed by genotyping as above,

190 and the presence of the ChR2 transgene was confirmed by rescue of the *lin-15(n765ts)* multi-
191 vulva (Muv) phenotype.
192
193 **HSN Channelrhodopsin strains**
194 ChR2 was expressed in the HSNs from the *egl-6* promoter via an integrated *wzIs30* transgene
195 (Emtage et al., 2012). This transgene was crossed into $G\alpha_q$ signaling mutants as follows. N2
196 males were crossed into LX1836 *wzIs30 IV; lite-1(ce314) lin-15(n765ts) X* to generate
197 heterozygous F1 males, which were then crossed separately into MIA211 *unc-73(ce362) I; lite-*
198 *1(ce314) lin-15(n765ts) X,* MIA299 *egl-30(ad805) I; lite-1(ce314) lin-15(n765ts) X*, MIA303 *egl-*
199 *8(n488) V; lite-1(ce314) lin-15(n765ts) X,* or MIA307 *egl-8(sa47) V; lite-1(ce314) lin-15(n765ts)*
200 *X* hermaphrodites to generate MIA247 *unc-73(ce362) I; wzIs30 IV; lite-1(ce314) X,* MIA300 *egl-*
201 *30(ad805) I; wzIs30 IV; lite-1(ce314) X*, MIA304 *wzIs30 IV; egl-8(n488)V; lite-1(ce314) X*, and
202 MIA308 *wzIs30 IV; egl-8(sa47) V; lite-1(ce314) X*. The presence of *lite-1(ce362)* was confirmed
203 by PCR genotyping, and the *wzIs30* transgene was confirmed by rescue of the *lin-15(n765ts)*
204 Muv phenotype.
205
206 **Behavior assays**
207 Quantification of egg accumulation was performed as described (Chase and Koelle, 2004).
208 Staged adults were obtained by picking late L4 animals and culturing them 24-30 h at 20°C.
209 Each animal was placed in 7 μL of 20% hypochlorite (bleach) solution and eggs were counted
210 after animals had dissolved. Numbers of eggs and any internally hatched L1 animals were
211 combined.
212
213 **Pharmacological assays**

214 Egg laying in response to exogenous serotonin was performed as described (Banerjee et al.,
215 2017; Kopchock et al., 2021). Individual staged adult animals were placed in 100 µl of either M9
216 buffer alone, or M9 containing 18.5 mM serotonin (creatinine sulfate monohydrate salt, Sigma-
217 Aldrich #H7752) or M9 containing 10 µM PMA (Phorbol-12-myristate-13-acetate, Calbiochem
218 #524400) in a 96-well microtiter dish. After 1 hour, the number of released eggs and L1 larvae
219 in each well were counted. Since egg-laying defective animals sometimes release one or two
220 eggs/L1 larvae in response to mechanical stimulation when they are first picked into the well,
221 animals were only recorded as responding if they laid 3 or more progeny. For calcium imaging,
222 NGM plates containing either PMA or ethanol solvent were prepared as described (Reynolds et
223 al., 2005). Age-matched adult worms from each genotype were placed on separate PMA or
224 control NGM plates at room temperature for 1.5 hour. An agar chunk was then placed between
225 two glass coverslips for Ca^{2+} activity recording as described (Ravi et al., 2018b). The unused
226 plates were kept at 4 °C for future use.
227
228 **Optogenetic assay**
229 All-*trans* retinal (Sigma Aldrich, R2500) was resuspended in ethanol (100%) to make 100 mM
230 solution and added to a warmed culture of OP50 bacteria grown in B Broth media to a final
231 concentration of 0.4 mM. Individual NGM agar plates were seeded with 200 µl of freshly
232 prepared +ATR food and were grown in the dark for ~24 hours prior to use. In all photo-
233 stimulation experiments, control animals were grown in the absence of ATR. Animals were
234 imaged at 4x magnification on a Leica M165FC stereomicroscope and illuminated with 3.3
235 mW/cm^2 of ~470 ± 20 nm blue light produced using a EL6000 metal halide light source and a
236 GFP excitation/emission filter set. The 30 s on/off sequence was programmed and controlled
237 using a Doric Optogenetics TTL Pulse Generator (OTPG-4, Version 3.3) triggering a SHB1
238 series shutter controller (ThorLabs; 170712-1).

239

240 **Microscopy**

241 **Ratiometric Ca^{2+} imaging**

242 Vulval muscle Ca^{2+} activity was performed in freely behaving adult animals at 24-30 h past the
243 late L4 larval stage, as described previously (Collins and Koelle 2013; Collins *et al.* 2016; Ravi
244 *et al.* 2018a). Worms co-expressing GCaMP5G and mCherry under the *unc-103e* promoter
245 transgene *vsIs164* were mounted beneath the chunk of agar over the glass slide. Ca^{2+} activity
246 was recorded through an 20X Apochromatic objective (0.8 NA) mounted on an inverted Zeiss
247 Axio Observer.Z1. A Colibri.2 LED illumination system was used to excite GCaMP5 at 470 nm
248 and mCherry at 590 nm for 10 msec every 50 msec. GFP and mCherry fluorescence emission
249 channels were separated using a Hamamatsu W-VIEW Gemini image splitter and recorded
250 simultaneously for 10 min with an ORCA-Flash 4.0 V2 sCMOS camera at 256 / 256-pixel
251 resolution (4x4 binning) at 16-bit depth. The motorized stage was manually controlled using a
252 joystick to maintain the freely behaving animal in the field of view. Image sequences were
253 exported to Volocity software (Quorum Technologies Inc.) for segmentation and ratiometric
254 analysis. Ca^{2+} transient peaks from ratio traces were detected using a custom MATLAB script,
255 as described (Ravi *et al.* 2018a).

256

257 **Experimental design and statistical analysis**

258 Sample sizes for behavioral assays followed previous studies (Chase and Koelle, 2004; Collins
259 et al., 2016). Statistical analysis was performed using Prism v.8 or v.9 (GraphPad). Ca^{2+}
260 transient peak amplitudes, widths, and inter-transient intervals were pooled from multiple
261 animals (typically ≥ 10 animals per genotype). All statistical tests were corrected for multiple
262 comparisons (Bonferroni for one-way ANOVA or Fisher's exact tests; Dunn's correction for

263 Kruskal–Wallis tests). Each figure legend indicates individual p-values with $p<0.05$ being
264 considered significant.
265
266

267 **Results**

268 **Trio RhoGEF acts both in neurons and muscle to drive egg-laying behavior**

269 Prior work has shown that $G\alpha_q$ signaling (Fig. 1A) through PLCβ and Trio RhoGEF promotes
270 neurotransmitter release and locomotion (Brundage et al., 1996; Miller et al., 1999; Williams et
271 al., 2007). How $G\alpha_q$ signaling regulates other *C. elegans* behavior circuits is less well
272 established. To address this uncertainty, we chose to examine the neural circuit driving egg-
273 laying behavior (Fig. 1B). Egg-laying behavior in *C. elegans* is regulated by a small motor circuit
274 with defined neurons and muscle connectivity (Cook et al., 2019; White et al., 1986). The HSNs
275 are serotonergic command motor neurons (Fig. 1B) that initiate the egg-laying active state and
276 promote the excitability of the vm1 and vm2 egg-laying vulval muscles (Collins et al., 2016;
277 Emtage et al., 2012; Waggoner et al., 1998). Innervating ventral cord neurons release
278 acetylcholine to regulate muscle contraction (Bany et al., 2003; Kim et al., 2001; Kopchock et
279 al., 2021; Waggoner et al., 2000). We first examined the steady-state accumulation of eggs in
280 the uterus as a proxy for changes in egg-laying circuit activity and behavior. As previously shown,
281 animals bearing mutations in the EAT-16 RGS protein, which inhibits $G\alpha_q$ signaling (Hajdu-
282 Cronin et al., 1999), or gain-of-function mutations in $G\alpha_q$ itself, (Bastiani et al., 2003; Doi and
283 Iwasaki, 2002) showed a significant increase in egg laying resulting in a significant reduction in
284 egg accumulation compared to the ~12 ± 3 embryos retained in wild-type animals (Fig. 1C-E;
285 Fig. 1I). Conversely, animals bearing mutations which reduce $G\alpha_q$ signaling showed the opposite
286 phenotype. Animals bearing an early nonsense mutation predicted to be a PLCβ null mutant,
287 *egl-8(sa47),* (Lackner et al., 1999; Williams et al., 2007) accumulated an average of 21 eggs, a
288 significant increase (Fig. 1G). Animals bearing a missense mutation in the RhoGEF domain of
289 Trio, *unc-73(ce362)* (Williams et al., 2007), showed an even stronger increase in egg
290 accumulation, accumulating 31 eggs and closely resembling animals bearing loss-of-function

291 mutations in $G\alpha_q$ itself (Fig. 1F-1I). Together, these results confirm that $G\alpha_q$ and its effectors
292 PLCβ and Trio RhoGEF are required for egg-laying behavior in *C. elegans* and that loss of the
293 Trio RhoGEF branch causes a stronger behavior impairment compared to loss of PLCβ.

294 Previous work has shown that PLCβ is expressed in neurons and in the intestine while
295 $G\alpha_q$ and Trio are expressed in nearly all excitable cells including neurons and muscles (Bastiani
296 et al., 2003; Brundage et al., 1996; Lackner et al., 1999; Miller et al., 1999; Steven et al., 1998).
297 To understand where $G\alpha_q$ and its effectors function to regulate egg laying, we used tissue-
298 specific promoters to express cDNAs encoding PLCβ or Trio RhoGEF in either all neurons, in
299 the body wall and egg-laying vulval muscles, or in both neurons and muscles. We found that
300 transgenic expression of PLCβ from a pan-neuronal promoter in PLCβ null mutants was
301 sufficient to rescue their defects in egg laying (Fig. 1J) and acetylcholine (ACh) release as
302 measured by restoration of sensitivity to aldicarb, a cholinesterase inhibitor (data not shown).
303 Previous work has indicated the presence of eight transcript variants of Trio (A, B, C1, C2, D1,
304 D2, E, and F), which are differentially expressed in *C. elegans* (Steven et al., 1998; Steven et
305 al., 2005). Transgenic expression of Trio RhoGEF-E in neurons is sufficient to rescue the
306 locomotion defects of Trio RhoGEF mutants (Williams et al., 2007). To explore whether Trio
307 RhoGEF acts similarly in neurons to promote egg laying, we used a pan-neuronal promoter to
308 express Trio RhoGEF-E and measured egg accumulation in these animals. We observed a
309 partial, but significant reduction in the number of eggs retained in Trio RhoGEF mutants (~36
310 eggs) compared to control Trio RhoGEF mutant animals (~42 eggs; Fig. 1K). In contrast,
311 transgenic expression of Trio RhoGEF-E in the egg-laying vulval muscles from a muscle-specific
312 promoter showed a much greater rescue of egg accumulation (~25 eggs), and this rescue of
313 egg laying was improved to nearly wild-type levels when Trio RhoGEF was expressed in both
314 neurons and muscles (~19 eggs; Fig. 1K). Together, these results confirm that $G\alpha_q$ effectors
315 PLCβ and Trio RhoGEF function in neurons to regulate egg-laying behavior. Our results also

316 suggest Trio RhoGEF also functions in the postsynaptic vulval muscles for proper regulation of
317 egg laying, a finding consistent with previously results regarding $G\alpha_q$ (Bastiani et al., 2003).
318
319 **Serotonin signals through $G\alpha_q$, Trio, and PLCβ to promote egg laying.**
320 Previous studies have shown that serotonin released from the HSNs signals through G-protein
321 coupled serotonin receptors expressed on the vulval muscles (Bastiani et al., 2003; Dempsey et
322 al., 2005; Fernandez et al., 2020; Tanis et al., 2008; Xiao et al., 2006). The vulval muscles are
323 also innervated by cholinergic ventral cord motor neurons (Cook et al., 2019; White et al., 1986)
324 whose release of ACh is regulated by serotonin and G protein signaling (Nurrish et al., 1999).
325 To test whether serotonin promotes egg laying via activating $G\alpha_q$ signaling, we measured the
326 egg-laying response to serotonin in $G\alpha_q$ signaling mutants. Serotonin promotes egg laying in
327 hypertonic M9 buffer, a condition that normally inhibits egg laying in both wild-type and HSNs-
328 deficient *egl-1(dm)* mutants, which developmentally lack the HSNs (Fig. 2B). Consistent with
329 previous results (Bastiani et al., 2003; Brundage et al., 1996; Trent et al., 1983), nearly 78% of
330 wild-type and 70% of HSN-deficient *egl-1(dm)* animals laid eggs in response to serotonin
331 compared to only 13% of $G\alpha_q$ mutant animals (Fig. 2B). Serotonin response was similarly and
332 significantly reduced to 23% and 3% in PLCβ and Trio RhoGEF mutant animals, respectively
333 (Fig. 2B). Our results are consistent with the previous results reporting that $G\alpha_q$ loss-of-function
334 mutants and PLCβ deletion null mutants, *egl-8(n488)* do not lay eggs in response to exogenous
335 serotonin (Bastiani et al., 2003; Trent et al., 1983). However, we find that a second PLCβ null
336 mutant *egl-8(sa47)* similarly fails to lay eggs in response to exogenous serotonin, a result
337 different from that previously reported (Bastiani et al., 2003). This discrepancy may arise from
338 somewhat different concentrations of serotonin used. The distinct responses of animals without
339 HSNs and animals lacking $G\alpha_q$ signaling indicate that $G\alpha_q$, PLCβ and Trio act at least in part

340 outside of HSNs to promote egg laying in response to serotonin. To determine where Trio
341 RhoGEF deficiency caused serotonin insensitivity, we measured egg laying in Trio RhoGEF
342 mutant animals re-expressing Trio RhoGEF-E in either neurons, muscles, or both. Transgenic
343 expression of Trio RhoGEF-E in neurons failed to rescue egg laying in response to serotonin
344 (Fig. 2C), but expression of Trio RhoGEF-E in muscles, or in both neurons and muscles, restored
345 egg laying of *unc-73(ce362)* mutant animals (Fig. 2C), suggesting Trio RhoGEF mediates
346 serotonin signaling in the vulval muscles. Together, these results indicate that $G\alpha_q$, PLCβ, and
347 Trio RhoGEF function at least in part outside of the HSNs to drive egg laying in response to
348 serotonin.
349

350 **Optogenetic stimulation of the HSNs and vulval muscles suggests cellular specificity of**
351 **$G\alpha_q$ effectors for egg-laying.**

352 Optogenetic stimulation of Channelrhodopsin-2 (ChR2) expressed in either the HSNs (Emtage
353 et al., 2012) or vulval muscles (Kopchock et al., 2021) can drive egg laying. To test whether and
354 how $G\alpha_q$ and its effectors mediate this response, we expressed ChR2 in HSNs in $G\alpha_q$ and
355 effector mutants and measured egg laying during 30s of exposure to blue light. Blue light
356 stimulation of the HSNs drove an average release of ~3 eggs in wild-type animals, which was
357 reduced to essentially zero in $G\alpha_q$ [(*egl-30(ad805)*] and Trio RhoGEF [*unc-73(ce362)*] mutants
358 (Fig. 3A), consistent to our previous results showing Trio RhoGEF acts in part in the postsynaptic
359 vulval muscles downstream of the HSNs. In contrast, optogenetic stimulation of the HSNs in
360 PLCβ null mutants [*egl-8(sa47)* or *egl-8(n488)*] drove robust egg release, releasing an average
361 of ~4 and ~6 embryos respectively in 30 s (Fig. 3A). The efficient rescue of egg laying in PLCβ
362 but not $G\alpha_q$ or Trio RhoGEF mutants upon optogenetic stimulation of HSNs is again consistent
363 with distinct $G\alpha_q$, PLCβ, and Trio RhoGEF requirements in the cells of the egg-laying circuit. To

364 test whether the failure of egg laying in $G\alpha_q$ and Trio RhoGEF mutants was a consequence of
365 muscle developmental defects, rather than excitability deficits, we expressed and stimulated
366 ChR2 in the vulval muscles. Blue light exposure drove the release of ~4 eggs in 30 s in wild-type
367 animals. Both PLCβ [*egl-8(sa47)* and *egl-8(nu488)*] and Trio RhoGEF mutants [*unc-73(ce362)*]
368 laid a similar number of eggs as wild-type control animals after blue light stimulation (Fig. 3B).
369 The *egl-30(ad805)* $G\alpha_q$ mutant laid slightly fewer eggs on average (~3) but this was not
370 significantly different than wild type. Thus, the failure of $G\alpha_q$ and Trio mutants to lay eggs in
371 response to exogenous serotonin or optogenetic stimulation of the HSNs does not arise from
372 some intrinsic defect in vulval muscle contractility, but rather a specific deficiency in muscle
373 excitability. These results are also consistent with prior findings showing rescue of egg-laying
374 behavior defects of $G\alpha_q$, PLCβ, and Trio RhoGEF mutants by exogenous phorbol esters
375 (Lackner et al., 1999; Williams et al., 2007). Together, these results support the conclusion from
376 our rescue experiments (Fig. 1J-1K) that PLCβ and Trio RhoGEF function in distinct cells and
377 through unique mechanisms to promote egg-laying circuit activity and behavior.
378

379 **$G\alpha_q$ and Trio RhoGEF are required for vulval muscle Ca^{2+} activity**

380 Egg laying in *C. elegans* is a two-state behavior where ~20 minute inactive states are punctuated
381 by ~2-minute active states with high levels of Ca^{2+} activity in the egg-laying circuit driving release
382 of 3-5 eggs (Collins et al., 2016; Waggoner et al., 1998; Zhang et al., 2008; Zhang et al., 2010).
383 Loss of $G\alpha_q$ signaling in *egl-30(n686)* animals causes a significant reduction in spontaneous and
384 serotonin-induced vulval muscle Ca^{2+} transients in immobilized animals (Shyn et al., 2003). We
385 therefore tested whether these $G\alpha_q$ dependent Ca^{2+} activity defects were shared in PLCβ and
386 Trio RhoGEF mutants. We expressed the genetically encoded Ca^{2+} reporter, GCaMP5, along
387 with mCherry in the vulval muscles of animals with either increased or decreased $G\alpha_q$ signaling

388 and performed ratiometric imaging in freely behaving animals. As shown in Figure 4A, the normal
389 two-state pattern of vulval muscle Ca^{2+} activity is lost in animals bearing strong loss-of-function
390 $G\alpha_q$ or Trio RhoGEF mutations. In both the *egl-30(ad805)* $G\alpha_q$ and *unc-73(ce362)* Trio mutants,
391 we failed to observe either the strong egg-laying Ca^{2+} transients where both the vm1 and vm2
392 muscles contract or even the smaller amplitude rhythmic 'twitch' Ca^{2+} transients (Fig. 4A) that
393 are localized to the vm1 muscles (Collins and Koelle, 2013), strongly reducing the observed Ca^{2+}
394 transient frequency (Fig. 4B). In contrast, the weaker *egl-30(n686)* $G\alpha_q$ mutant and two different
395 PLCβ null mutants showed grossly normal vulval muscle Ca^{2+} activity during both egg-laying
396 and twitch transients (Fig. 4A-C). The elevated pattern of vulval muscle Ca^{2+} activity we
397 observed in weak *egl-30(n686)* $G\alpha_q$ and PLCβ mutants resembled *egl-1(dm)* animals lacking
398 the HSNs (Collins et al., 2016). These animals still enter and leave infrequent egg-laying active
399 states, possibly driven by the accumulation of eggs in the uterus (Ravi et al., 2018a). DAG
400 Kinase-θ (DGK-θ) is thought to reduce DAG signaling through conversion to phosphatidic acid
401 (Fig. 1A). Loss of the DGK-θ/DGK-1 increases neurotransmitter release and egg laying, likely
402 through elevation of DAG levels and activation of downstream effectors (Jose and Koelle, 2005;
403 Miller et al., 1996; Nurrish et al., 1999). To test if *dgk-1* mutants have increased egg-laying
404 muscle activity, we performed Ca^{2+} imaging in *dgk-1(nu62)* mutants. Somewhat surprisingly,
405 DAG Kinase mutant animals did not show a significant increase in vulval muscle Ca^{2+} activity
406 (Fig. 4A-C). Like PLCβ, DGK-1 is expressed in neurons (Nurrish et al., 1999), suggesting
407 alterations of IP_3 and /or DAG levels in neurons may affect the frequency of egg-laying active
408 states without altering the overall pattern or strength of vulval muscle Ca^{2+} activity within those
409 active states. Indeed, *goa-1(n1134)* mutants that reduce inhibitory $G\alpha_o$ signaling have
410 hyperactive egg-laying behavior defects that strongly resemble *dgk-1(nu62)* mutants without
411 causing a correspondingly significant increase in vulval muscle Ca^{2+} activity (Ravi et al., 2021)

412 Conversely, animals with increased $G\alpha_q$ signaling either from a gain-of-function *egl-30(tg26)*
413 mutations or *eat-16(tm761)* null mutations showed a significant increase in the amplitude of
414 vulval muscle Ca^{2+} transients (Fig. 4A and 4C). We also observed a significant increase in the
415 frequency of vulval muscle Ca^{2+} transients in *egl-30(tg26)* mutants, but this was not shared in
416 *eat-16(tm761*) mutants. Together, these results indicate $G\alpha_q$ and Trio RhoGEF, but not PLCβ,
417 promote vulval muscle activity that drives twitching and egg-laying Ca^{2+} transients during egg-
418 laying active states.
419

420 **DAG mimetics restore muscle activity and egg laying to $G\alpha_q$ signaling mutants**

421 How does serotonin signaling through $G\alpha_q$ promote vulval muscle activity? Previous results have
422 shown that DAG mimetic phorbol esters restore locomotion and animal viability to $G\alpha_q$ null
423 mutants and restore egg laying in PLCβ, Trio RhoGEF double mutants (Williams et al., 2007).
424 However, the effects of phorbol esters on egg laying in single mutants was not clear, raising
425 questions as to whether PMA rescued egg laying downstream of PLCβ, Trio RhoGEF, or both
426 (Fig. 5A). We measured the egg-laying responses of wild-type animals and $G\alpha_q$ signaling
427 mutants to Phorbol 12-myristate 13-acetate (PMA). As shown in Figure 5B, PMA treatment
428 strongly stimulated egg laying in wild-type animals and all mutants with reduced $G\alpha_q$ signaling
429 (≥80% animals laying eggs). Like serotonin (Fig. 2B), PMA also rescued egg laying in *egl-1(dm)*
430 mutant animals lacking the HSNs (Fig. 4B), but only PMA rescued egg laying in $G\alpha_q$ and effector
431 signaling mutants. These results are consistent with PMA acting downstream of both serotonin
432 release from the HSNs and its subsequent signaling through $G\alpha_q$. We next imaged how
433 exogenous PMA affected vulval muscle Ca^{2+} transient activity. We performed 10-minute
434 GCaMP5 Ca^{2+} recordings of wild-type or $G\alpha_q$ signaling mutants treated for two hours with 10 μM
435 PMA (Movies 1-3). Quantitation of Ca^{2+} transients showed that PMA significantly increased

436 vulval muscle Ca^{2+} activity in wild-type animals to 10±1.6 transients per minute from an average
437 2±0.9 transients per min in vehicle-treated, wild-type animals (Fig. 5C-D and Movie 1). PMA also
438 restored both rhythmic twitch and egg-laying Ca^{2+} transients to strong $G\alpha_q$ and Trio RhoGEF
439 signaling mutants, with Ca^{2+} transients frequencies increasing from essentially 0±0.8 transients
440 per minute in vehicle-treated controls to 7±2 transients per minute after PMA treatment, almost
441 but not quite to the level of PMA-treated wild-type control animals (Fig. 5C-D and Movies 2-3).
442 Together, these studies show that DAG-mimetic phorbol esters restore muscle excitability and
443 contractility defects of $G\alpha_q$ and Trio RhoGEF mutants, suggesting DAG production is a major
444 and necessary consequence of both $G\alpha_q$ and Trio RhoGEF signaling.
445
446 **DAG promotes egg laying independent of UNC-13 and Protein Kinase C**
447 How do phorbol esters such as PMA rescue vulval muscle Ca^{2+} activity and egg laying? Previous
448 results have shown that DAG and PMA bind to C1 domain-containing proteins such as mUNC-
449 13/UNC-13 and Protein Kinase C (PKC) to regulate their activity (Betz et al., 1998; Huang, 1989;
450 Konig et al., 1985; Newton, 2001; Silinsky and Searl, 2003).To test if DAG regulates egg-laying
451 behavior through activation of UNC-13 or PKC, we tested how PMA and serotonin affect egg
452 laying in mutants lacking these proteins (Fig. 6). Mutants that eliminate axonal and synaptic
453 UNC-13 show reduced egg laying, accumulating an average of 22 eggs compared to 15 seen in
454 wild-type animals (Fig. 6A). Null *unc-13(s69)* and loss of function *unc-13(e51)* mutants have
455 much less severe egg-laying defects compared to $G\alpha_q$ signaling mutants, accumulating ~22 and
456 ~19 eggs (Fig. 6A) compared to >30 eggs (Fig. 1C-I). These results suggest that $G\alpha_q$ promotes
457 synaptic transmission and egg-laying through an UNC-13 independent pathway. If PMA
458 activation of vulval muscle Ca^{2+} and egg laying were mediated by UNC-13, then mutations that
459 eliminate this protein should reduce that response. However, *unc-13* mutants still laid eggs in

460 response to PMA (Fig. 6B). Because DAG production may be a conserved biochemical
461 consequence of $G\alpha_q$ signaling through both PLCβ and Trio RhoGEF pathways, and both effector
462 pathways have functions in neurons, we hypothesized that serotonin might promote egg laying
463 via modulation of UNC-13 activity. In support of this model, *unc-13* mutants failed to lay eggs in
464 response to serotonin (Fig. 6B). To determine whether serotonin promotes egg laying through
465 Protein Kinase C, we analyzed egg accumulation in animals bearing predicted null mutations in
466 different PKC isoforms (Edwards et al., 2012; Hyde et al., 2011; Okochi et al., 2005; Tabuse,
467 2002; Tabuse et al., 1989). PKC-1 has previously been shown to promote neuropeptide
468 transmission (Sieburth et al., 2007). While neuropeptides signal to promote egg laying (Avery et
469 al., 1993; Brewer et al., 2019; Jacob and Kaplan, 2003; Kass et al., 2001), PKC-1 (nPKC-ε) null
470 mutants showed a grossly normal egg accumulation of 14~17 eggs (Fig. 6C). Animals bearing
471 predicted null mutants of novel and conventional PKCs such as nPKCδ/θ (TPA-1) and cPKCα/β
472 (PKC-2) orthologs also show no significant differences in egg accumulation (Fig. 6C), suggesting
473 that disruption of PKC signaling does not strongly affect egg-laying behavior. Like UNC-13, If
474 PMA activation of vulval muscle Ca^{2+} and egg laying were mediated by PKCs, then mutations
475 that eliminate PKCs, should reduce that response. However, PKC single mutant animals still laid
476 eggs in response to PMA (Fig. 6C). Together, these results support a model where serotonin
477 promotes neurotransmitter release and egg laying via UNC-13, however, there are additional
478 targets of DAG that function in parallel to UNC-13 in neurons and/or downstream of UNC-13 in
479 the vulval muscles to promote egg laying.
480

481 **Discussion**

482 In this study we explored the cellular specificity of $G\alpha_q$ effector signaling as it regulates egg-
483 laying circuit activity and behavior using molecular genetics, optogenetics, pharmacology, and
484 calcium imaging techniques. We found that $G\alpha_q$ effectors PLCβ and Trio RhoGEF differentially
485 act in neurons and muscles to promote synaptic transmission and egg-laying behavior. PLCβ
486 signals presynaptically in neurons while Trio RhoGEF signals both presynaptically in neurons
487 and postsynaptically in muscles. Although $G\alpha_q$, PLCβ, and Trio RhoGEF mutants all fail to lay
488 eggs in response to serotonin, optogenetic stimulation of HSNs fully rescued egg laying in PLCβ
489 but not $G\alpha_q$ or Trio RhoGEF mutants, suggesting hyperactivation of the HSNs may be able to
490 bypass PLCβ signaling in some cases. Recent work has shown that the HSNs release NLP-3
491 neuropeptides which can promote egg laying even in *tph-1* mutants lacking serotonin (Brewer
492 et al., 2019), possibly explaining why optogenetic activation of HSNs may be able to stimulate
493 egg laying in PLCβ mutants even when exogenous serotonin cannot. The HSNs are also
494 predicted to release Ach (Gendrel et al., 2016; Pereira et al., 2015), which may signal through
495 nAChR receptors expressed on the vulval muscles (Kim et al., 2001; Waggoner et al., 2000).
496 Because serotonin drives egg laying in animals lacking HSNs but not in animals lacking PLCβ,
497 we propose that $G\alpha_q$ and PLCβ act in neurons other than HSN to promote ACh release onto the
498 vulval muscles for egg laying. The cholinergic VA, VB, and VC neurons also innervate the vulval
499 muscles alongside the HSNs (Cook et al., 2019; White et al., 1986). Consistent with this model,
500 we have recently shown that blocking VC synaptic transmission reduces egg laying in response
501 to serotonin (Kopchock et al., 2021). Optogenetic stimulation of the VCs (Kopchock et al., 2021)
502 or VA/VB neurons (Kopchock et al., unpublished) stimulates vulval muscle Ca^{2+} activity, but the
503 resulting Ca^{2+} activity is insufficient to drive egg laying behavior (data now shown). Because we
504 find that mutations that increase $G\alpha_q$ signaling have stronger vulval muscle Ca^{2+} transients, we

505 propose that serotonin and NLP-3 released from HSN potentiates both ACh release from other
506 motor neurons and the electrical excitability and/or contractility of the vulval muscles, converting
507 rhythmic twitch Ca^{2+} transients into stronger egg-laying transients. Previous studies have shown
508 that Trio RhoGEF acts in presynaptic motor neurons to regulate locomotion behavior (Hu et al.,
509 2011; Steven et al., 2005; Williams et al., 2007). Our studies show that transgenic Trio RhoGEF
510 expression in either neurons or muscles alone is insufficient to restore wild-type level of egg-
511 laying behavior, but expression in both is sufficient. These results mirror previously published
512 results for $G\alpha_q$ (Bastiani et al., 2003), further supporting a model where PLCβ and Trio RhoGEF
513 have distinct functions during locomotion and egg-laying behaviors.

514 How do $G\alpha_q$, PLCβ and Trio-RhoGEF signaling promote egg-laying behavior? Earlier
515 studies have suggested that Rho ortholog RHO-1 in *C. elegans* regulates synaptic activity in a
516 mechanism that involves the G12 family protein GPA-12 (Hiley et al., 2006; Lutz et al., 2005).
517 Activated RHO-1 also directly binds to and inhibits the DGK-1 diacylglycerol kinase expressed
518 in neurons that signals to reduce DAG available to bind effectors (Hiley et al., 2006; McMullan
519 et al., 2006). Our data are consistent with the previous results reporting that $G\alpha_q$ signaling
520 regulates postsynaptic vulval muscle activity mainly through $G\alpha_q$-Trio pathway as $G\alpha_q$, and Trio
521 mutants show a similarly strong reduction in vulval muscle Ca^{2+} activity. Because muscle activity
522 defects in $G\alpha_q$ and Trio mutants can be restored by the DAG-mimetic PMA, we suggest that
523 insufficient levels of DAG are responsible for the circuit activity and behavior defects of $G\alpha_q$ and
524 Trio RhoGEF mutants. In the absence of PLCβ, how would parallel $G\alpha_q$ signaling through Trio
525 RhoGEF and RHO-1 generate DAG? Besides PLCβ (EGL-8), *C. elegans* expresses four other
526 PLC orthologs: PLCε (PLC-1), PLC-2, PLCγ (PLC-3), and PLCδ (PLC-4) (Vázquez-Manrique et
527 al., 2008). *In vitro* studies with cultured mammalian cells show that small G proteins like Rho can
528 bind to and activate PLCε (Seifert et al., 2008; Wing et al., 2003). Genetic evidence in *C. elegans*

529 suggests a model that both PLCε and PLCγ likely function downstream of $G\alpha_q$ to promote cell
530 activity (Kunitomo et al., 2013; Yu et al., 2013), but whether Trio activation of Rho ultimately acts
531 through these PLCs to produce DAG is not clear. One approach to test if these other PLCs
532 mediate Rho signaling would be to perform genetic epistasis experiments. However, loss of Rho-
533 1 causes lethality (Jantsch-Plunger et al., 2000; McMullan and Nurrish, 2011) and loss of PLCε
534 and PLCγ cause sterility defects (Yin et al., 2004), limiting our ability to measure differences in
535 egg laying. Imaging or biochemical experiments documenting changes in PIP_2 (Stauffer et al.,
536 1998) and/or DAG (Ohno et al., 2017; Tewson et al., 2012) could allow for directs tests of
537 whether $G\alpha_q$ signaling through Trio and Rho changes PIP2 and DAG levels *in vivo*.

538 Previous studies have shown that the DAG mimetic phorbol esters promote both synaptic
539 vesicle and dense core vesicle release from neurons and neurosecretory cells (Silinsky and
540 Searl, 2003). DAG and phorbol esters activate many effectors including mUNC-13 in the brain
541 and Protein Kinase C (PKC) in nearly all cells (Betz et al., 1998; Huang, 1989). In *C. elegans*,
542 treatment of exogenous PMA promotes hypersensitivity to the paralytic effects of aldicarb
543 (Sieburth et al., 2007). Double mutants of both PKC-1 null and UNC-13 (H17K) show a greater
544 magnitude of resistivity to phorbol esters compared to either mutant alone suggesting that PMA
545 acts in part through these effectors to regulate ACh release (Sieburth et al., 2007; Silinsky and
546 Searl, 2003). Our data show that animals lacking either UNC-13 or single PKC isoforms still
547 show a robust egg-laying response to PMA (Fig. 6), suggesting DAG and PMA promote muscle
548 activity via other targets. *In vitro* studies show ROCK (Rho-associated coiled-coil kinase)
549 activation in PMA-induced apoptosis and macrophage differentiation (Chang et al., 2006; Yang
550 et al., 2017). ROCK has a predicted C1 domain that mediates protein interaction with DAG and
551 might bind and be similarly activated by PMA (Xiao et al., 2009). In *C. elegans,* RHO-1 signals
552 through LET-502/ROCK to phosphorylate non-muscle myosin light chain (Shimizu et al., 2018).
553 $G\alpha_q$ also promotes neurotransmitter release via additional kinase targets including SEK-1

554 Mitogen-Activated Protein Kinase Kinase in the p38 MAPK pathway and KSR-1 in the ERK
555 MAPK pathway (Coleman et al., 2018; Hoyt et al., 2017). KSR-1 is particularly interesting in that
556 its N-terminus shares sequence similarly with C1 domains that might mediate regulation by DAG.
557 Loss of KSR-1 and other ERK MAPK components also suppress the loopy locomotion defects
558 caused by gain-of-function mutations in Rho-1 (Coleman et al., 2018). Taken together, our work
559 is consistent with a model where additional DAG-sensitive effectors act downstream of $G\alpha_q$, Trio
560 and Rho to promote muscle excitability and /or contractility for egg laying.

561 Apart from direct activation of C1 domain containing effectors, emerging evidence
562 indicates Phospholipase C-dependent production of DAG can regulate neural circuit activity via
563 endocannabinoid-mediated retrograde signaling. In pyramidal cells of the mouse hippocampus,
564 postsynaptic calcium influx through voltage-gated calcium channels activates PLCβ1 to
565 generate DAG (Hashimotodani et al., 2006; Hashimotodani et al., 2007; Soltesz et al., 2015).
566 Diacylglycerol lipase-α (DAGLα) can convert DAG to Arachidonoylglycerol (2-AG), which signals
567 from dendrites in a retrograde manner through presynaptic $G\alpha_o$-coupled endocannabinoid
568 receptors to inhibit neurotransmitter release (Hashimotodani et al., 2013; Hashimotodani et al.,
569 2005; Soltesz et al., 2015; Tanimura et al., 2010; Wettschureck et al., 2006). In *C. elegans*, 2-
570 AG activates the NPR-19 endocannabinoid receptor ortholog that couples to $G\alpha_o$ to modulate
571 serotonin transmission, pharyngeal, feeding, and locomotory behaviors (Oakes et al., 2019;
572 Oakes et al., 2017; Pastuhov et al., 2016). We have recently shown that feedback of egg
573 accumulation alters vulval muscle Ca^{2+} activity, which subsequently signals to regulate bursts of
574 Ca^{2+} transients in the HSNs that accompany the onset of the egg-laying active state (Ravi et al.,
575 2018a; Ravi et al., 2021), These results support a model where stretch-dependent feedback of
576 egg accumulation stimulates postsynaptic vulval muscle Ca^{2+} signaling. This Ca^{2+} could then
577 activate PLCs to generate DAG and 2-AG which signal to modulate HSN activity, serotonin
578 release, and egg laying. The genetic and experimental accessibility of the *C. elegans* egg-laying

579 circuit should allow us to determine if conserved G proteins like $G\alpha_q$ act generally to drive neural
580 circuit activity via changes in DAG, subsequent activation of effectors, and retrograde
581 messengers like 2-AG.
582
583

584 **Acknowledgements**

585 This work was funded by grants from the NIH (R01-NS086932) and NSF (IOS-1844657) to KMC.
586 PD is supported by AHA predoctoral fellowship Award (20PRE35210233). We thank Drs.
587 Kenneth Miller and Joshua Kaplan for sharing plasmids and strains. Some of the strains used in
588 this study were provided by the *C. elegans* Genetics Center, which is funded by NIH Office of
589 Research Infrastructure Programs (P40 OD010440). We thank Drs. Julia Dallman, Laura
590 Bianchi, and Athula Wikramanayake along with members of the Collins lab for helpful
591 discussions and feedback on the manuscript.

592

A

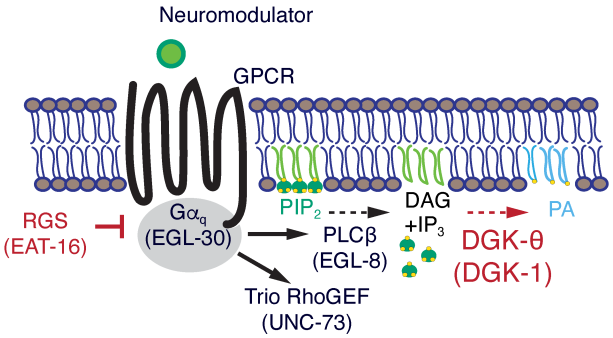
Neuromodulator
GPCR
RGS
(EAT-16)
Gαq
(EGL-30)
PIP2
DAG
+IP3
PA
PLCβ
(EGL-8)
DGK-θ
(DGK-1)
Trio RhoGEF
(UNC-73)

B

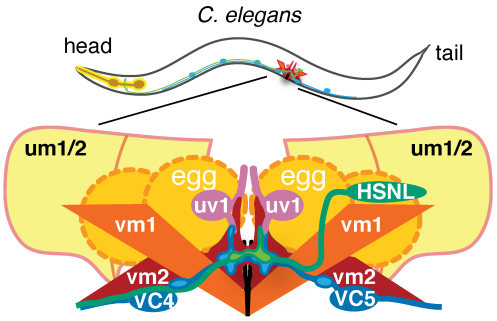
C. elegans
head
tail
um1/2
um1/2
egg
egg
uv1
uv1
HSNL
vm1
vm1
vm2
VC4
vm2
VC5

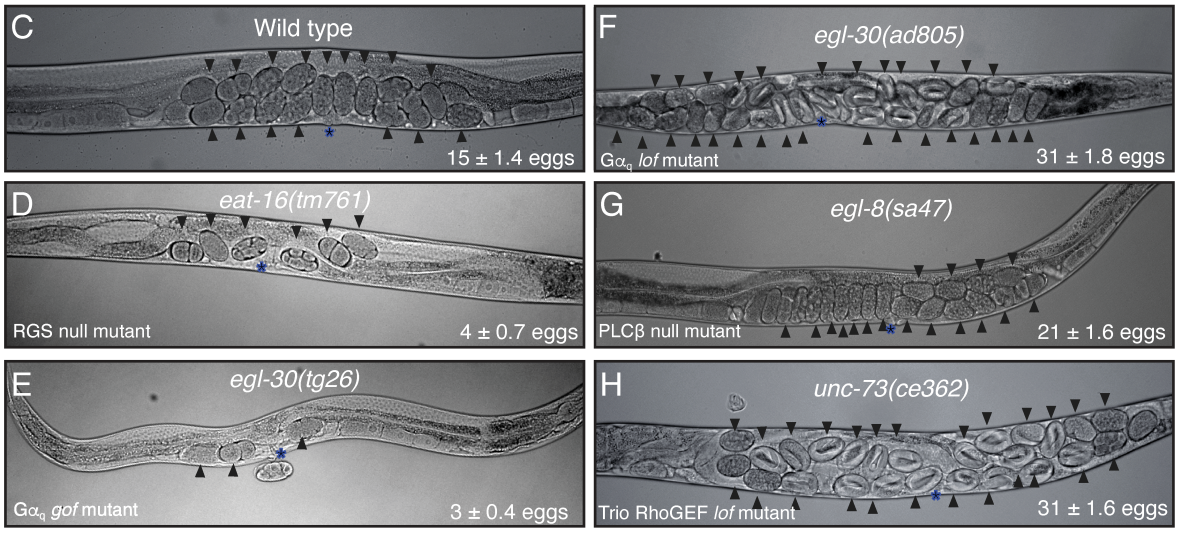
C
Wild type
15 ± 1.4 eggs
D
eat-16(tm761)
RGS null mutant
4 ± 0.7 eggs
E
egl-30(tg26)
Gαq gof mutant
3 ± 0.4 eggs
F
egl-30(ad805)
Gαq lof mutant
31 ± 1.8 eggs
G
egl-8(sa47)
PLCβ null mutant
21 ± 1.6 eggs
H
unc-73(ce362)
Trio RhoGEF lof mutant
31 ± 1.6 eggs

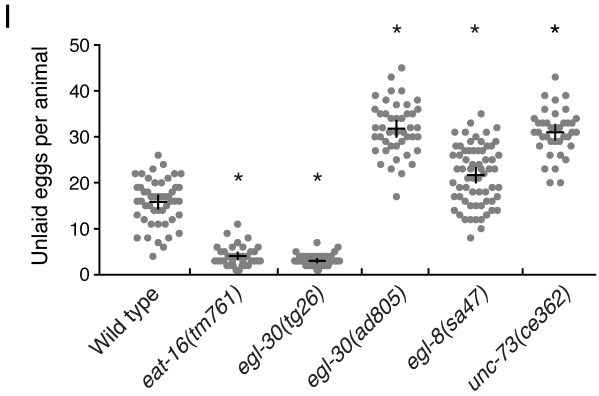
I
Unlaid eggs per animal
0
10
20
30
40
50
Wild type
eat-16(tm761)
egl-30(tg26)
egl-30(ad805)
egl-8(sa47)
unc-73(ce362)

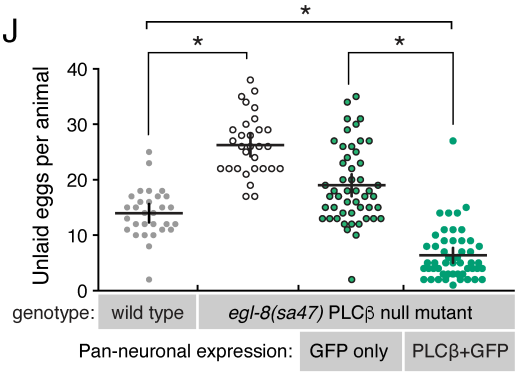
J
Unlaid eggs per animal
0
10
20
30
40
genotype:
wild type
egl-8(sa47) PLCβ null mutant
Pan-neuronal expression:
GFP only
PLCβ+GFP

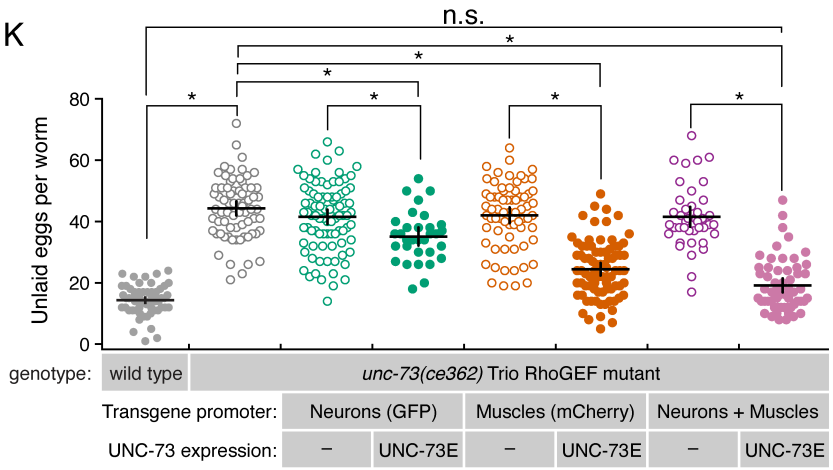
K
n.s.
Unlaid eggs per worm
0
20
40
60
80
genotype:
wild type
unc-73(ce362) Trio RhoGEF mutant
Transgene promoter:
Neurons (GFP)
Muscles (mCherry)
Neurons + Muscles
UNC-73 expression:
–
UNC-73E
–
UNC-73E
–
UNC-73E

593 **Figure 1: Trio RhoGEF is required in both neurons and muscles to regulate egg-laying**
594 **behavior (A)** Schematics of excitatory (black) and inhibitory (red) $G\alpha_q$ signaling pathway. *C.*
595 *elegans* gene names are beneath the protein they encode. **(B)** Cartoon of the *C. elegans* egg-
596 laying behavior circuit from a lateral view. Only the left side of the bilaterally symmetric circuit is
597 shown. HSNL, Hermaphrodite Specific Neuron (left); VC4 and VC5 Ventral C neurons; vm1 and
598 vm2 vulval muscles, um1 and um2 uterine muscles; uv1 uterine-vulval neuroendocrine cells. **(C-**
599 **H)** Bright field images of worms of the indicated genotypes; arrowheads indicate accumulated
600 eggs. Mean number of accumulated eggs ± 95% confidence intervals is also indicated. Position
601 of the vulva is shown with asterisk (*). **(I)** Scatterplot of egg accumulation in wild-type, *eat-*
602 *16(tm761)*, *egl-30(tg26)*, *egl-30(ad805), egl-8(sa47), and unc-73(ce362)* mutant animals. Line
603 indicates mean eggs ± 95% confidence intervals. Asterisks indicate p ≤0.0001 (One way ANOVA
604 with Bonferroni's correction; wild type (n=49); *eat-16(tm761)* (n=36); *egl-30(tg26)* (n=47); *egl-*
605 *30(ad805)* (n=44); *egl-8(sa47)* (n=65); *unc-73(ce362)* (n=38). **(J)** Transgenic rescue of *egl-8*
606 PLCβ egg-laying defects. Scatterplot of egg accumulation in transgenic animals expressing GFP
607 only or EGL-8/PLCβ fused to GFP from the *rgs-1* promoter in *egl-8(sa47)* null mutants (n=50)
608 compared to wild-type (n=30) and *egl-8(sa47)* mutant animals (n=30). Bar indicates mean eggs
609 ±95% confidence intervals. Asterisks indicate p≤0.0001 (One-way ANOVA with Bonferroni's
610 correction) **(K)** Transgenic rescue of *unc-73* Trio RhoGEF egg-laying defects. Scatterplot of egg
611 accumulation in wild-type (n=60), *unc-73(ce362)* mutants (n=72), and transgenic animals
612 expressing a fluorescent protein with or without Trio in neurons (n≥32) or in muscles (n≥69), or
613 in both neurons and muscles (n≥41) in *unc-73(ce362)* mutants. Horizontal line indicates mean
614 accumulated eggs ±95% confidence intervals. Asterisks indicate p≤0.0145; n.s.= not significant
615 (p>0.05; One-way ANOVA with Bonferroni's correction for multiple comparisons).

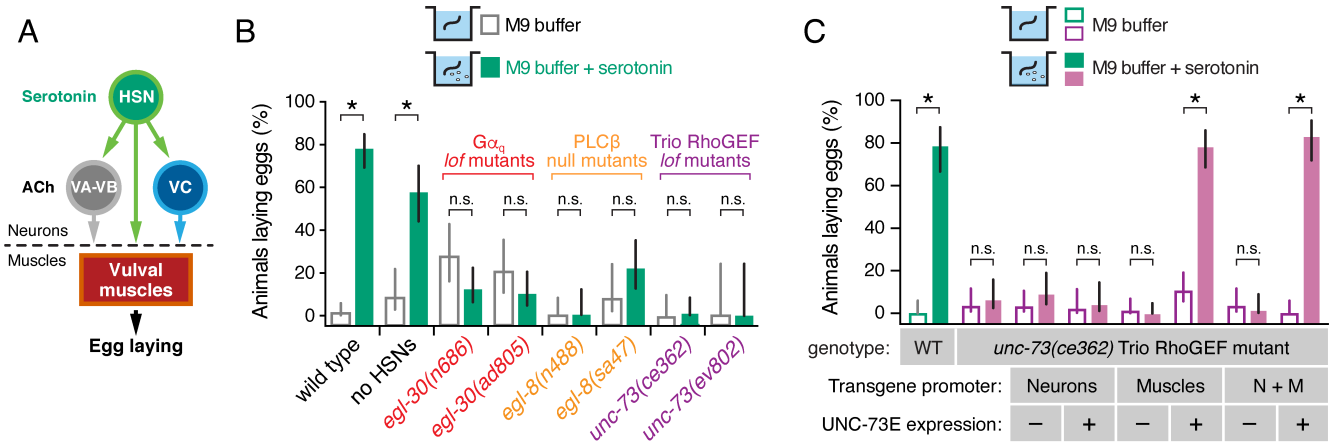

Figure 2: Serotonin signals through Gα$_q$, Trio, and PLCβ to promote egg-laying. **(A)** Model of serotonergic and acetylcholine (ACh) signaling in the egg-laying circuit. **(B)** Bar plots showing the percentage of animals laying eggs in M9 buffer alone (grey) or M9 +18.5 mM serotonin (green) in 1 hr. Bar indicates mean percent ±95% confidence intervals. Asterisks indicate p<0.0007; n.s.= not significant (p>0.05, Fisher's exact test with Bonferroni's correction for multiple comparisons; n>30 animals). **(C)** Bar plot showing percent of animals laying eggs in M9 buffer or M9 +18.5 mM serotonin in wild-type or Trio RhoGEF mutant animals expressing nothing or Trio RhoGEF in neurons, muscles, or both. Bar indicates mean percent ±95% confidence intervals. Asterisks indicate p<0.0007; n.s.= not significant (p>0.05, Fisher's exact test with Bonferroni's correction for multiple comparisons; n>30 animals).

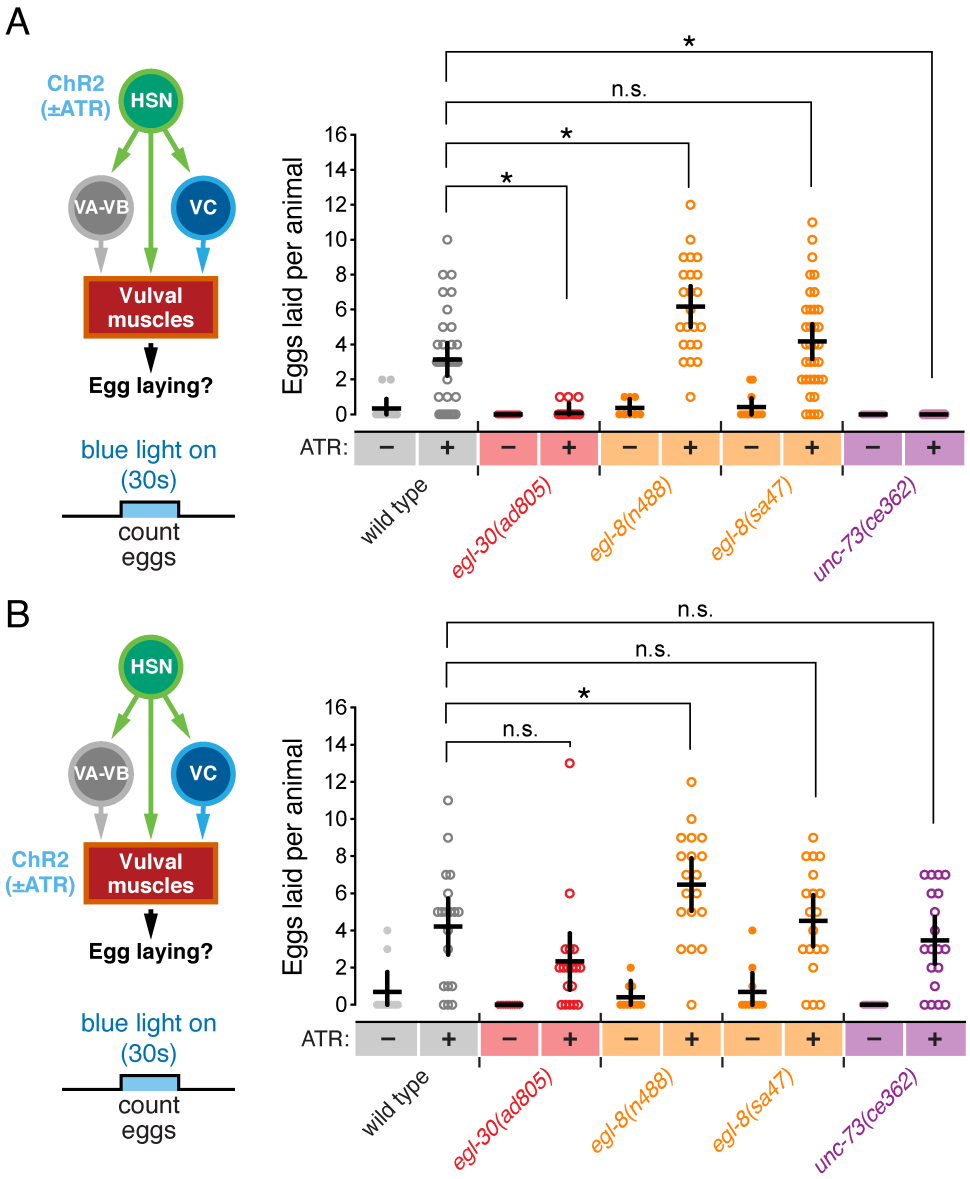

Figure 3: Optogenetic stimulation of the HSNs or vulval muscles indicates cellular specificity of Gα_q effectors for egg laying. (A) On left, cartoon of the egg-laying circuit and experiment showing blue light activation of HSN for 30 seconds. On right, scatterplot showing eggs laid per worm in presence (+) or absence (-) of all-*trans* retinal (ATR) cofactor during the blue light activation of ChR2 expressed in HSNs of wild-type (grey), *egl-30(ad805)* Gα_q strong loss-of-function mutants (red), *egl-8(n488) and egl-8(sa47)* PLCβ mutants (orange), and *unc-73(ce362)* Trio mutant (purple) animals. Line indicates mean eggs laid ±95% confidence

636 intervals. Asterisks indicate $p<0.0001$; n.s.= not significant ($p>0.05$, One-way ANOVA with
637 Bonferroni's correction for multiple comparisons; n= how many animals?). (**B)** On the left,
638 cartoon of the egg-laying circuit and experiment showing blue light activation of vulval muscles
639 for 30 seconds(left). On the right, scatter plots of eggs laid per worm in presence (+) or absence
640 (-) of ATR during blue light activation of ChR2 expressed in the vulval muscles of wild type, *egl-*
641 *30(ad805)* $G\alpha_q$ strong loss-of-function mutants (red), *egl-8(n488) and egl-8(sa47)* PLCβ mutants
642 (orange)*,* and *unc-73(ce362)* Trio mutant (purple) animals. Line indicates mean eggs laid ±95%
643 confidence intervals. Asterisk indicates $p\leq0.0255$; n.s.=not significant, $p>0.05$ (One-way ANOVA
644 with Bonferroni's correction for multiple comparisons; $n>10$).

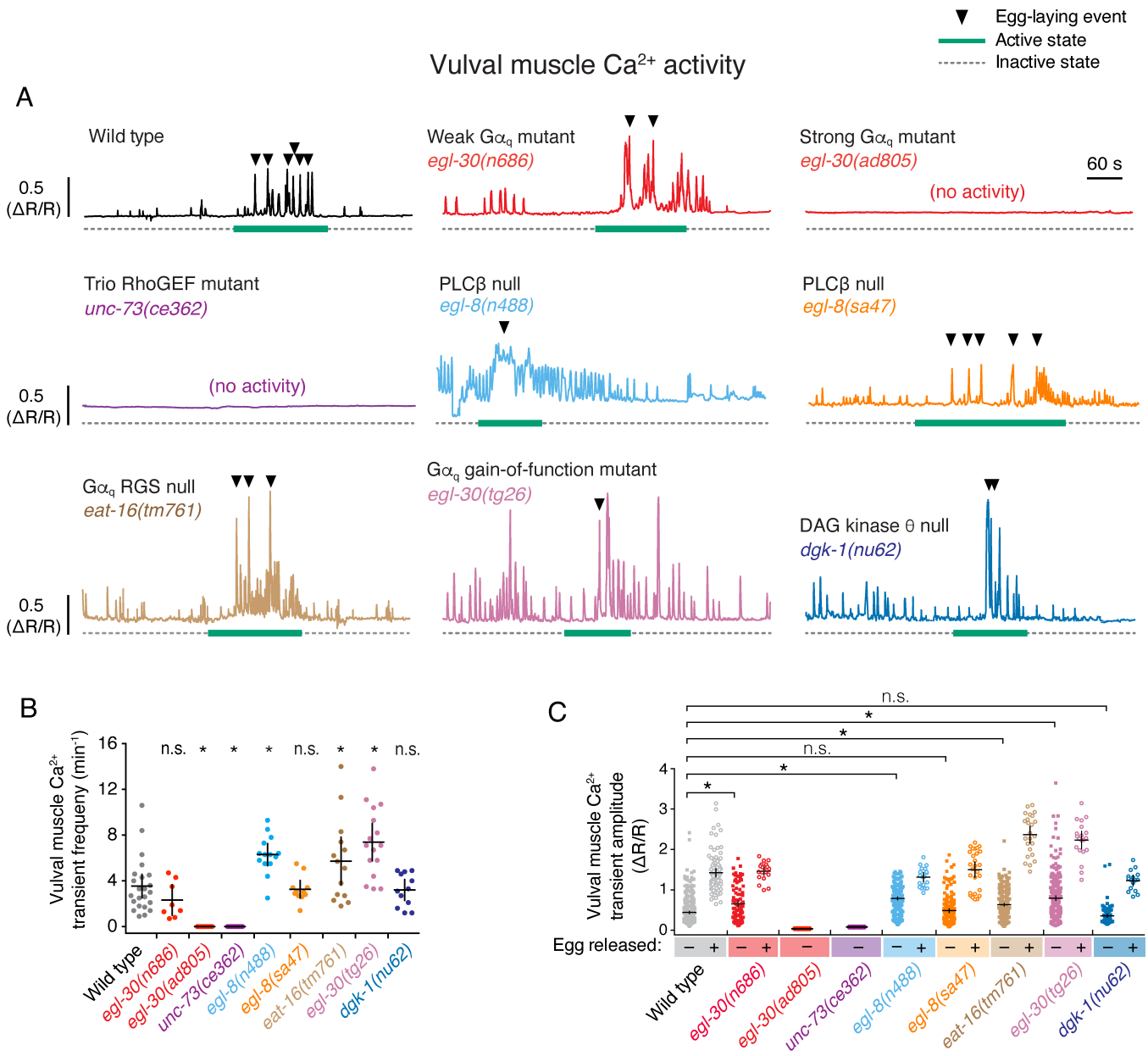

Figure 4: Gαq and Trio signaling promotes vulval muscle activity. (A) Representative GCaMP5::mCherry (ΔR/R) ratio traces showing vulval muscle Ca^{2+} activity in freely behaving wild-type (black), *egl-30(n686)* Gαq weak loss of function mutant (red), *egl-30(ad805)* Gαq strong loss-of-function mutant (red), *unc-73 (ce362)* Trio strong loss-of-function mutant (purple), *egl-8(n488)* PLCβ null mutant (light blue), *egl-8(sa47)* PLCβ null mutant (orange), *eat-16(tm761)* Gαq RGS protein null mutant (grey), *egl-30(tg26)* strong Gαq gain-of-function mutant (magenta), and *dgk-1(nu62)* DAG Kinase null mutant *(*dark blue*)* animals during active (green solid bar) and

653 inactive (dotted grey line) egg-laying behavior states. Arrowheads indicate egg-laying events.
654 Vertical and horizontal scale bars show GCaMP5/mCherry fluorescence ratio (ΔR/R) and time,
655 respectively **(B)** Scatterplots of Ca^{2+} transient frequency for indicated genotypes. Line indicates
656 mean eggs laid ±95% confidence intervals; asterisks indicate $p \leq 0.0340$; n.s. indicates not
657 significant ($p > 0.05$, One-way ANOVA with Bonferroni's correction for multiple comparisons;
658 $n > 10$ animals recorded per genotype). **(C)** Scatterplots of Ca^{2+} peak amplitudes for the indicated
659 genotypes during twitch (closed square) and egg-laying transients (open circles). Asterisks
660 indicate $p < 0.0001$, n.s. indicates not significant ($p > 0.05$, Kruskal Wallis test with Dunn's
661 correction for multiple comparisons).

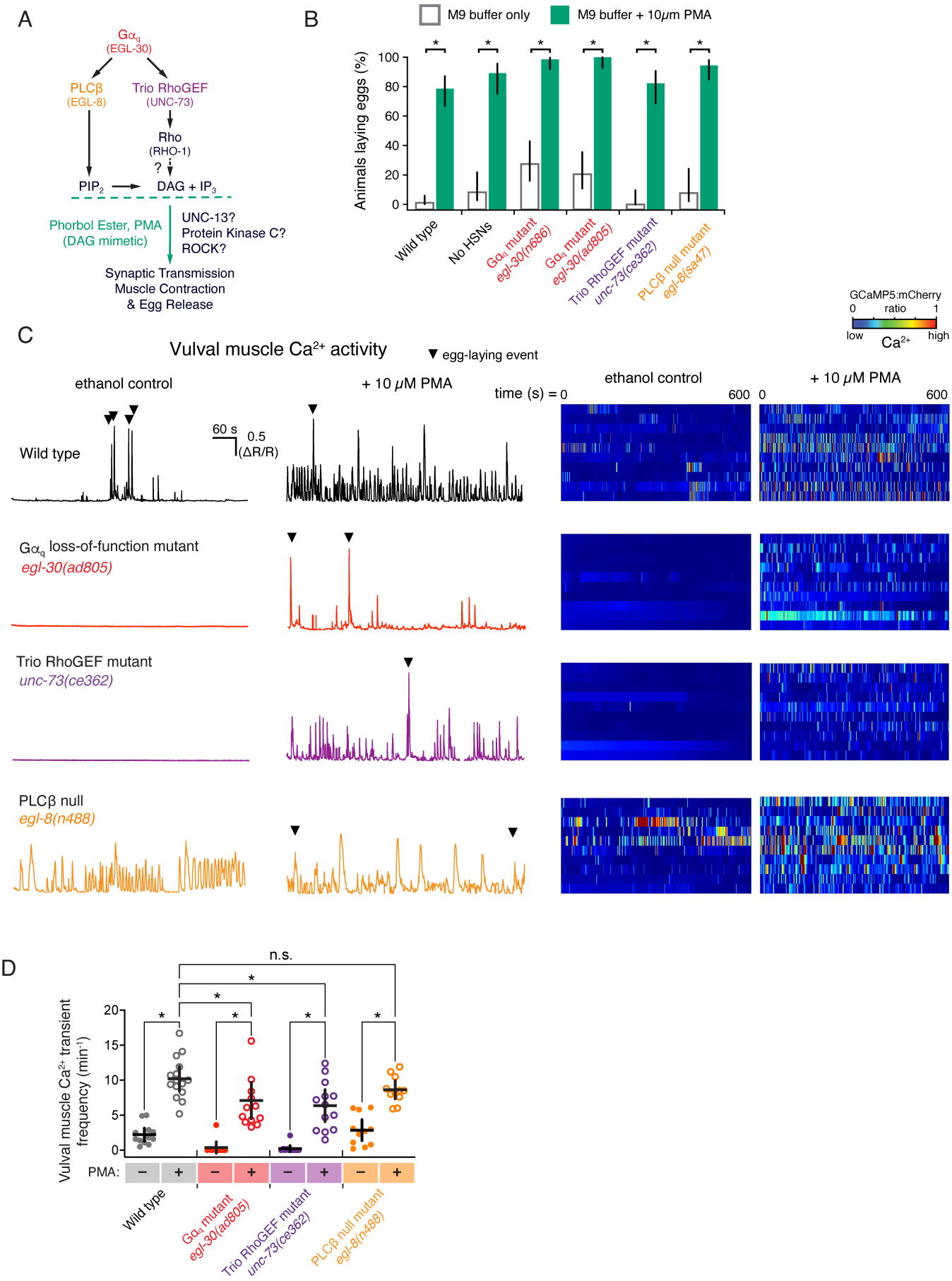
A
Gαq
(EGL-30)
PLCβ
(EGL-8)
Trio RhoGEF
(UNC-73)
Rho
(RHO-1)
?
PIP2
DAG + IP3
Phorbol Ester, PMA
(DAG mimetic)
UNC-13?
Protein Kinase C?
ROCK?
Synaptic Transmission
Muscle Contraction
& Egg Release
B
M9 buffer only
M9 buffer + 10μm PMA
Animals laying eggs (%)
100
80
60
40
20
0
Wild type
No HSNs
Gαq mutant
egl-30(n686)
Gαq mutant
egl-30(ad805)
Trio RhoGEF mutant
unc-73(ce362)
PLCβ null mutant
egl-8(sa47)
GCaMP5:mCherry
0 ratio 1
low Ca2+ high
C
Vulval muscle Ca2+ activity
egg-laying event
ethanol control
+ 10 μM PMA
time (s) = 0 600
ethanol control
+ 10 μM PMA
0 600
Wild type
60 s
0.5
(ΔR/R)
Gαq loss-of-function mutant
egl-30(ad805)
Trio RhoGEF mutant
unc-73(ce362)
PLCβ null
egl-8(n488)
D
n.s.
Vulval muscle Ca2+ transient
frequency (min-1)
20
15
10
5
0
PMA:
−
+
Wild type
Gαq mutant
egl-30(ad805)
Trio RhoGEF mutant
unc-73(ce362)
PLCβ null mutant
egl-8(n488)

662

663 **Figure 5: DAG mimetic PMA rescues egg-laying circuit activity and behavior defects of**
664 **$G\alpha_q$ signaling mutants**. **(A)** Diagrams showing working model of $G\alpha_q$ and DAG signaling
665 pathway during egg-laying behavior. **(B)** Bar plots showing the percentage of animals showing
666 egg laying in M9 buffer (open grey bars) or M9 buffer +10 μM PMA (filled green bars) Sample
667 size for each genotype and each condition. Error bars indicate 95% confidence intervals for the
668 proportion; asterisks indicate $p<0.0006$ (Fisher's exact test with Bonferroni's correction for
669 multiple comparisons; $n\geq30$ animals per genotype and condition). **(C)** Left, representative
670 GCaMP5::mCherry (ΔR/R) ratio traces showing vulval muscle Ca^{2+} activity in wild-type or the
671 indicated $G\alpha_q$ signaling mutant animals in the absence or presence of 10 μM PMA. Arrowheads
672 indicate egg-laying events. Vertical and horizontal scale bars show GCaMP5/mCherry
673 fluorescence ratio (ΔR/R) and time, respectively. Right, heat map showing intensity modulated
674 color spectrum of GCaMP5::mCherry (ΔR/R) ratio of vulval muscle Ca^{2+} activity ranging from
675 blue (low Ca^{2+}) to red (high Ca^{2+}) of 10 animals. **(D)** Scatterplots of Ca^{2+} transient frequency in
676 the absence (-) and presence (+) of 10 μM PMA for the indicated genotypes. Line indicates mean
677 eggs laid ±95% confidence intervals; asterisk indicates $p\leq0.0275$; n.s.= not significant ($p>0.05$,
678 One-way ANOVA with Bonferroni's correction for multiple comparisons; $n\geq10$ animals per
679 genotype and condition).
680

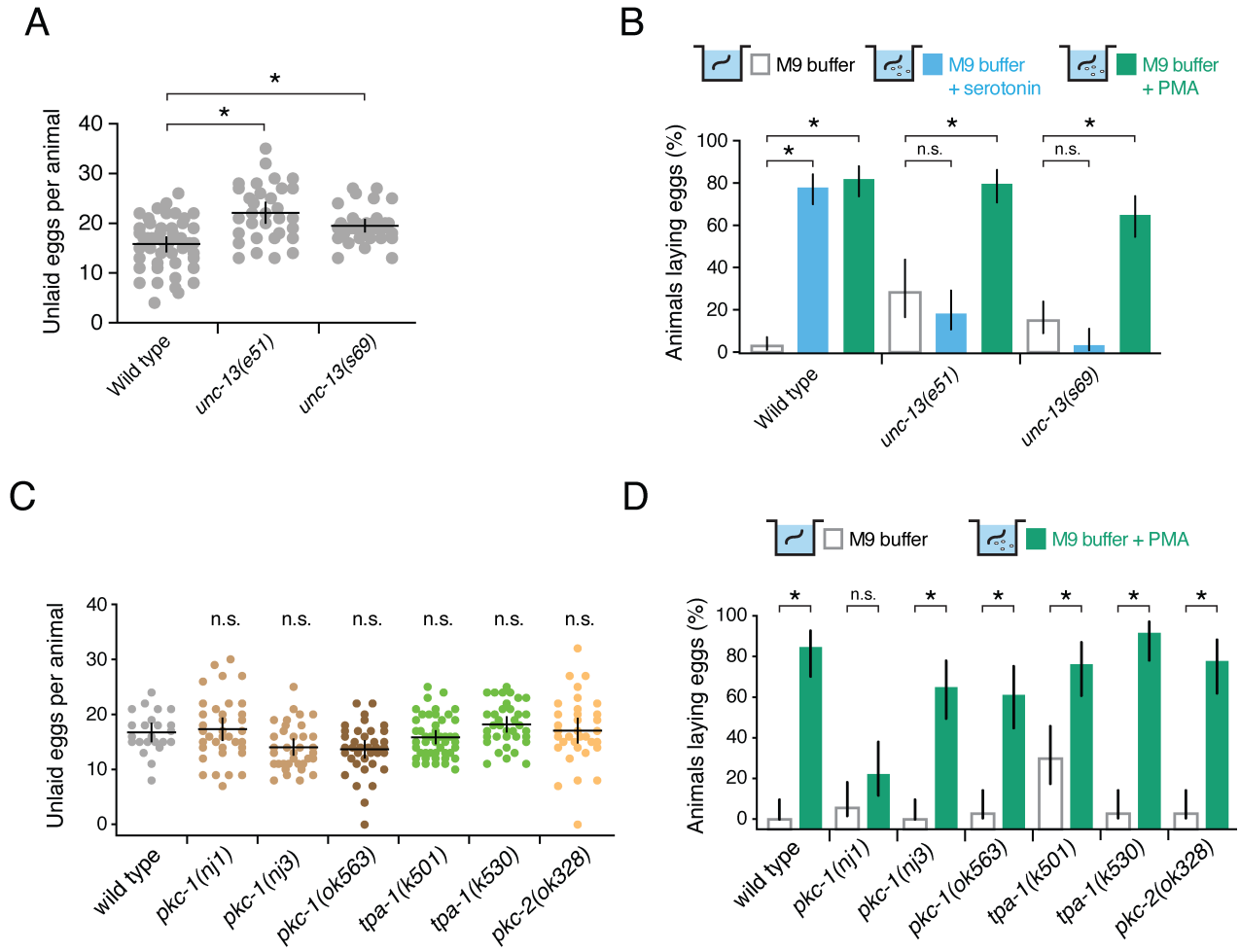

Figure 6: DAG promotes egg laying independent of UNC-13 or Protein Kinase C. (A) Scatterplot of egg accumulation in wild-type, *unc-13(e51)* loss-of-function mutant, and *unc-13(s69)* null mutant animals. Line indicates mean eggs laid ±95% confidence intervals. Asterisk indicates p ≤0.0021 (One-way ANOVA with Bonferroni's correction for multiple comparisons; n≥36 per genotype and condition). (**B)** Bar plots showing the percentage of wild-type, *unc-13(e51),* or *unc-13(s69)* mutant animals laying eggs in M9 buffer (grey open boxes), 18.5 mM serotonin (filled blue boxes), or 10 μM PMA (filled green boxes). Bar indicates mean eggs ±95% confidence interval for the proportion. Asterisks indicate p<0.0006; n. s = not significant (p>0.05, Fisher's exact test with Bonferroni's correction for multiple comparisons; n≥36 animals per genotype and condition). **(C)** Scatterplot of egg accumulation in wild-type (n=24) and indicated Protein Kinase C mutant animals (n≥35 per genotype). Line indicates average eggs accumulated

693 ±95% confidence intervals. n.s.= not significant ($p>0.05$, One-way ANOVA with Bonferroni's
694 correction for multiple comparisons **(D)** Bar plots showing the percentage of wild-type and
695 Protein Kinase C mutant animals showing egg laying in M9 buffer (open bars) or 10 μM PMA
696 (filled green bars). Bar indicates mean eggs ±95% confidence intervals for the proportion.
697 Asterisks indicate $p<0.0007$; n.s.= not significant ($p>0.05$, Fisher's exact test with Bonferroni
698 correction for multiple comparisons; $n\geq35$ animals per genotype and condition).
699

700 **Movie 1: GCaMP5:mCherry fluorescence ratio in the vulval muscles of wild-type animals**
701 **in the absence or presence of 10 μM DAG analogue, PMA.** Blue indicates low Ca^{2+}, and red
702 indicates elevated Ca^{2+}.
703
704 **Movie 2: GCaMP5:mCherry fluorescence ratio in the vulval muscles of strong loss of**
705 **function $G\alpha_q$ mutant, *egl-30(ad805),* in the absence or presence of 10 μM DAG analogue,**
706 **PMA.** Blue indicates low Ca^{2+}, and red indicates elevated Ca^{2+}.
707
708 **Movie 3: GCaMP5:mCherry fluorescence ratio in the vulval muscles of strong loss of**
709 **function Trio mutant, *unc-73(ce362)*, animals in the absence or presence of PMA.** Blue
710 indicates low Ca^{2+}, and red indicates elevated Ca^{2}.
711
712 **Table 1: Lists of *C. elegans* strains used in this study**
713

Strains	Genotype	Feature	Figure(s)	Source
N2	Wild type	Bristol wild-type strain	1,2,5	(Brenner, 1974)
MT1434	*egl-30(n686) I*	$G\alpha_q$ loss-of-function mutant, Egg-laying defective	1,2,5	(Trent et al., 1983)
DA823	*egl-30(ad805) I*	$G\alpha_q$ strong loss-of-function mutant, Egg-laying defective	1,2,5	(Brundage et al., 1996; Mendel et al., 1995)
KG1278	*unc-73(ce362) I*	Trio RhoGEF loss-of-function mutant, Egg-laying defective	1,2	(Williams et al., 2007)

KG1397	*unc-73(ev802) I*	Trio RhoGEF deletion mutant, Egg-laying defective	2,5	(Williams et al., 2007)
JT47	*egl-8(sa47) V*	PLCβ null, Egg-laying defective	1,2,5	(Thomas, 1990)
MT1083	*egl-8(n488) V*	PLCβ null, Egg-laying defective	2	(Trent et al., 1983)
LX1226	*eat-16(tm761) I*	$G\alpha_q$ RGS null, Hyperactive egg laying	1	(Porter and Koelle, 2010)
CG21	*egl-30(tg26) I; him-5(e1490) V*	$G\alpha_q$ gain-of-function mutant, Hyperactive egg-laying	1	(Garcia et al., 2001)
LX1832	*lite-1(ce314) lin-15(n765ts) X*	strain used for transgenic line creation		(Gürel et al., 2012)
LX1286	*egl-8(sa47) I; lin-15(n765ts) X*	PLCβ null mutant, Egg-laying defective; multi-vulva	1	This study
LX1674	*egl-8(sa47) I; lin-15(n765ts) X; vsEx679*	PLCβ null, Egg-laying defective; non-Muv, expresses GFP in neurons from *rgs-1* promoter	1	This study
LX1675	*egl-8(sa47) I; lin-15(n765ts) X; vsEx680*	PLCβ null, Egg laying defective; non-Muv, expresses PLCβ and GFP in neurons from *rgs-1* promoter	1	This study
MIA26	*egl-1(n986dm) V*	Lacks HSNs	2,5	(Ravi et al., 2018a)
LX1918	*vsIs164 lite-1(ce314) lin-15(n765ts) X*	Expresses GCaMP5 and mCherry in the vulval muscles	4,5	(Li et al., 2013)

MIA109	*egl-8(sa47) V; vsIs164 lite-1(ce314), lin-15(n765ts) X*	Expresses GCaMP5 and mCherry in the vulval muscles of *egl-8(sa47)* mutant	4,5	This study
MIA139	*egl-30(n686) I; vsIs164 lite-1(ce314) lin-15(n765ts) X*	Expresses GCaMP5 and mCherry in the vulval muscles of *egl-30(n686*)	4,5	This study
MIA140	*egl-30(ad805) I; vsIs164 lite-1(ce314), lin-15(n765ts) X*	Expresses GCaMP5 and mCherry in the vulval muscles of *egl-30(ad805)*	4,5	This study
MIA141	*unc-73(ce362) I; vsIs164, lite-1(ce314) lin-15(n765ts) X*	Expresses GCaMP5 and mCherry in the vulval muscles of *unc-73(ce362)*	4,5	This study
MIA286	*egl-30(tg26) I; vsIs164, lite-1(ce314) lin-15(n765ts) X*	Expresses GCaMP5 and mCherry in the vulval muscles of *egl-30(tg26)*	4	This study
MIA287	*eat-16(tm761) I; vsIs164 lite-1(ce314) lin-15(n765ts) X*	Expresses GCaMP5 and mCherry in the vulval muscles of *eat-16(tm761)*	4	This study

MIA288	*egl-8(n488) V; vsIs164 lite-1 (ce314) lin-15(n765ts) X*	Expresses GCaMP5 and mCherry in the vulval muscles of *egl-8(n488)*	4,5	This study
MIA296	*dgk-1(nu62) lite-1(ce314) lin-15(n765ts) X*	Expresses GCaMP5 and mCherry in the vulval muscles of *dgk-1(nu62)*	4	This study
MIA372	*unc-73(ce362) I; keyEx64*	Expresses GFP in the neurons and mCherry in the muscles of *unc-73(ce362)*	1	This study
MIA373	*unc-73(ce362) I; keyEx65*	Expresses GFP and Trio RhoGEF-E cDNA in the neurons, and mCherry and Trio RhoGEF-E cDNA in the muscles of *unc-73(ce362)*	1	This study
MIA374	*unc-73(ce362) I; keyEx66*	Expresses GFP in neurons	1	This study
MIA375	*unc-73(ce362) I; keyEx67*	Expresses GFP and Trio RhoGEF-E cDNA in neurons	1	This study
MIA376	*unc-73(ce362) I; keyEx68*	Expresses mCherry in muscles	1,2	This study
MIA377	*unc-73(ce362) I; keyEx69*	Expresses mCherry and Trio RhoGEF-E cDNA in muscles	1,2	This study

LX1836	*wzIs30 IV; lite-1(ce314) lin-15(n765ts) X*	Expresses Channelrhodopsin-2 (ChR2) in HSNs from the *egl-6* promoter	3	(Collins et al., 2016)
MIA229	*keyIs48; lite-1(ce314) lin-15(n765ts) X*	Expresses ChR2 in vulval muscles from the *ceh-24* promoter	3	(Kopchock et al., 2021)
MIA300	*egl-30(ad805) I; wzIs30 IV; lite-1(ce314) X*	Expresses ChR2 in HSN of *egl-30(ad805)* mutant	3	This study
MIA301	*egl-30(ad805) I; keyIs48; lite-1(ce314) X*	Expresses ChR2 in vulval muscles of *egl-30(ad805)* mutant	3	This study
MIA304	*wzIs30 IV; egl-8(n488) V; lite-1(ce314) X*	Expresses ChR2 in HSNs of *egl-8(n488)* mutant	3	This study
MIA305	*egl-8(n488) V; keyIs48; lite-1(ce314) X*	Expresses ChR2 in vulval muscles of *egl-8(n488)* mutant	3	This study
MIA308	*wzIs30 IV; egl-8(sa47) V; lite-1(ce314) X*	Express ChR2 in HSNs of *egl-8(sa47)* mutant	3	This study
MIA309	*egl-8(sa47) V; keyIs48; lite-1(ce314) X*	Expresses ChR2 in vulval muscles of *egl-8(sa47)* mutant	3	This study

MIA247	*unc-73(ce362) I; wzIs30 IV; lite-1(ce314) X*	Expresses ChR2 in HSN of *unc-73(ce362)* mutant	3	This study
MIA248	*unc-73(ce362) I; keyIs48; lite-1(ce314) X*	Expresses ChR2 in vulval muscles of *unc-73(ce362)* mutant	3	This study
MT7929	*unc-13(e51) I*	UNC-13 loss-of-function	6	(Brenner, 1974)
EG9631	*unc-13(s69) I*	UNC-13 null	6	(Rose and Baillie, 1980)
IK105	*pkc-1(nj1) V*	nPKCε null	6	(Okochi et al., 2005)
IK130	*pkc-1(nj3) V*	nPKCε null	6	(Okochi et al., 2005)
RB781	*pkc-1(ok563) V*	nPKCε null	6	(Consortium, 2012)
VC127	*pkc-2(ok328) X*	cPKCα/β null	6	(Consortium, 2012)
MJ500	*tpa-1(k501) IV*	nPKCδ/θ null	6	(Tabuse et al., 1989)
MJ563	*tpa-1(k530) IV*	nPKCδ/θ null	6	(Tabuse et al., 1989)

714

715

716 **Table 2: Lists of oligonucleotide sequences used in this study**

Oligo Name	Sequence (5'>3')	Use
lite-1(ce314)-fwd	ACGGGAGACGAAGAGCTAAATAGG	Genotyping of *lite-1(ce314)*
lite-1(ce314)-rev	CTAAGTTGCCGGTTGCCTTAGAAC	Genotyping of *lite-1(ce314)*
egl-30(n686)-F	GCCAACCGAGCAGGACATTCTGCG	Genotyping of *egl-30(n686)*
eg-30(n686)-R	CGGGAAAGTAGTCAGCGAGATGCG	Genotyping of *egl-30(n686)*
egl-30(ad805)-F	GCCAGGGCTGTCCCATTACGG	Genotyping of *egl-30(ad805)*
egl-30(ad805)-R	TCGGAAAGCGCCACCAGGAAC	Genotyping of *egl-30(ad805)*
egl-8-cDNA-fwd	CTTGGCTAGCGTAGAAAAAATGGCAAAGGAGTTCCAGTTC	For amplification of *egl-8* coding sequences
egl-8-cDNA-rev	CGCCCATGGTTATCAAACGACAGAAGTCGGTTGAGC	For amplification of *egl-8* coding sequences
egl-8-Cterm-NotI-fwd	GTGGGTACTCCACTGGGGGTGCGGCCGCTGGAGGTCCTTCGACACCGGT	Quick change mutagenesis of *egl-8* cDNA to insert in-frame NotI enzyme for GFP insertion
egl-8-Cterm-NotI-rev	ACCGGTGTCGAAGGACCTCCAGCGGCCGCACCCCCAGTGGAGTACCCAC	Quick-change mutagenesis of *egl-8* cDNA to insert in-frame NotI enzyme for GFP insertion

NotI-GFP-FWD	GGTGCGGCCGCTGGAAGTAAA GGAGAAGAACTTTTC	For amplification of GFP with flanking, in-frame NotI enzyme sites for insertion into *egl-8* cDNA
NotI-GFP-REV	TCCAGCGGCCGCTCCTTTGTAT AGTTCATCCATGCC	For amplification of GFP with flanking, in-frame NotI enzyme sites for insertion into *egl-8* cDNA
RE-GFP-FWD-new	GCGTCTAGAACCGGTGCTAGC GTAGAAAAAATGGTCAGTAAAG GAGAAGAACTTTTC	For amplification of sequences encoding GFP for cloning into pGP3 *rgs-1* promoter containing plasmid
RE-GFP-REV	TACGAATTCGGTACCTCAGATT TATTTGTATAGTTCATCCATG	For amplification of sequences encoding GFP for cloning into pGP3 *rgs-1* promoter containing plasmid

717

718 **References:**

719 Akerboom, J., Carreras Calderon, N., Tian, L., Wabnig, S., Prigge, M., Tolo, J., Gordus, A., Orger, M.B.,
720 Severi, K.E., Macklin, J.J., *et al.* (2013). Genetically encoded calcium indicators for multi-color
721 neural activity imaging and combination with optogenetics. Front Mol Neurosci *6*, 2.

722 Ananthanarayanan, B., Stahelin, R.V., Digman, M.A., and Cho, W. (2003). Activation mechanisms of
723 conventional protein kinase C isoforms are determined by the ligand affinity and conformational
724 flexibility of their C1 domains. J Biol Chem *278*, 46886-46894.

725 Avery, L., Bargmann, C.I., and Horvitz, H.R. (1993). The Caenorhabditis elegans unc-31 gene affects
726 multiple nervous system-controlled functions. Genetics *134*, 455-464.

727 Banerjee, N., Bhattacharya, R., Gorczyca, M., Collins, K.M., and Francis, M.M. (2017). Local
728 neuropeptide signaling modulates serotonergic transmission to shape the temporal organization
729 of C. elegans egg-laying behavior. PLoS Genet *13*, e1006697.

730 Bany, I.A., Dong, M.Q., and Koelle, M.R. (2003). Genetic and cellular basis for acetylcholine inhibition of
731 Caenorhabditis elegans egg-laying behavior. J Neurosci *23*, 8060-8069.

732 Bastiani, C.A., Gharib, S., Simon, M.I., and Sternberg, P.W. (2003). Caenorhabditis elegans Galphaq
733 regulates egg-laying behavior via a PLCbeta-independent and serotonin-dependent signaling
734 pathway and likely functions both in the nervous system and in muscle. Genetics *165*, 1805-
735 1822.

736 Berridge, M.J., Lipp, P., and Bootman, M.D. (2000). The versatility and universality of calcium signalling.
737 Nat Rev Mol Cell Biol *1*, 11-21.

738 Betke, K.M., Wells, C.A., and Hamm, H.E. (2012). GPCR mediated regulation of synaptic transmission.
739 Prog Neurobiol *96*, 304-321.

740 Betz, A., Ashery, U., Rickmann, M., Augustin, I., Neher, E., Sudhof, T.C., Rettig, J., and Brose, N. (1998).
741 Munc13-1 is a presynaptic phorbol ester receptor that enhances neurotransmitter release.
742 Neuron *21*, 123-136.
743 Brenner, S. (1974). The genetics of Caenorhabditis elegans. Genetics *77*, 71-94.
744 Brewer, J.C., Olson, A.C., Collins, K.M., and Koelle, M.R. (2019). Serotonin and neuropeptides are both
745 released by the HSN command neuron to initiate Caenorhabditis elegans egg laying. PLoS Genet
746 *15*, e1007896.
747 Brose, N., and Rosenmund, C. (2002). Move over protein kinase C, you've got company: alternative
748 cellular effectors of diacylglycerol and phorbol esters. J Cell Sci *115*, 4399-4411.
749 Brundage, L., Avery, L., Katz, A., Kim, U.J., Mendel, J.E., Sternberg, P.W., and Simon, M.I. (1996).
750 Mutations in a C. elegans Gqalpha gene disrupt movement, egg laying, and viability. Neuron *16*,
751 999-1009.
752 Chang, Y.C., Lee, H.H., Chen, Y.J., Bokoch, G.M., and Chang, Z.F. (2006). Contribution of guanine
753 exchange factor H1 in phorbol ester-induced apoptosis. Cell Death Differ *13*, 2023-2032.
754 Chase, D.L., and Koelle, M.R. (2004). Genetic analysis of RGS protein function in Caenorhabditis
755 elegans. Methods Enzymol *389*, 305-320.
756 Chhatriwala, M.K., Betts, L., Worthylake, D.K., and Sondek, J. (2007). The DH and PH domains of Trio
757 coordinately engage Rho GTPases for their efficient activation. J Mol Biol *368*, 1307-1320.
758 Coleman, B., Topalidou, I., and Ailion, M. (2018). Modulation of Gq-Rho Signaling by the ERK MAPK
759 Pathway Controls Locomotion in Caenorhabditis elegans. Genetics *209*, 523-535.
760 Collins, K.M., Bode, A., Fernandez, R.W., Tanis, J.E., Brewer, J.C., Creamer, M.S., and Koelle, M.R.
761 (2016). Activity of the C. elegans egg-laying behavior circuit is controlled by competing activation
762 and feedback inhibition. Elife *5*.

763 Collins, K.M., and Koelle, M.R. (2013). Postsynaptic ERG potassium channels limit muscle excitability to
764 allow distinct egg-laying behavior states in Caenorhabditis elegans. J Neurosci *33*, 761-775.
765 Consortium, C.e.D.M. (2012). large-scale screening for targeted knockouts in the Caenorhabditis
766 elegans genome. G3 (Bethesda) *2*, 1415-1425.
767 Cook, S.J., Jarrell, T.A., Brittin, C.A., Wang, Y., Bloniarz, A.E., Yakovlev, M.A., Nguyen, K.C.Q., Tang, L.T.,
768 Bayer, E.A., Duerr, J.S.*, et al.* (2019). Whole-animal connectomes of both Caenorhabditis elegans
769 sexes. Nature *571*, 63-71.
770 Dempsey, C.M., Mackenzie, S.M., Gargus, A., Blanco, G., and Sze, J.Y. (2005). Serotonin (5HT),
771 fluoxetine, imipramine and dopamine target distinct 5HT receptor signaling to modulate
772 Caenorhabditis elegans egg-laying behavior. Genetics *169*, 1425-1436.
773 Doi, M., and Iwasaki, K. (2002). Regulation of retrograde signaling at neuromuscular junctions by the
774 novel C2 domain protein AEX-1. Neuron *33*, 249-259.
775 Dong, M.Q., Chase, D., Patikoglou, G.A., and Koelle, M.R. (2000). Multiple RGS proteins alter neural G
776 protein signaling to allow C. elegans to rapidly change behavior when fed. Genes Dev *14*, 2003-
777 2014.
778 Edwards, M.R., Johnson, J.R., Rankin, K., Jenkins, R.E., Maguire, C., Morgan, A., Burgoyne, R.D., and
779 Barclay, J.W. (2012). PKC-2 phosphorylation of UNC-18 Ser322 in AFD neurons regulates
780 temperature dependency of locomotion. J Neurosci *32*, 7042-7051.
781 Emtage, L., Aziz-Zaman, S., Padovan-Merhar, O., Horvitz, H.R., Fang-Yen, C., and Ringstad, N. (2012).
782 IRK-1 potassium channels mediate peptidergic inhibition of Caenorhabditis elegans serotonin
783 neurons via a G(o) signaling pathway. J Neurosci *32*, 16285-16295.

784 Fernandez, R.W., Wei, K., Wang, E.Y., Mikalauskaite, D., Olson, A., Pepper, J., Christie, N., Kim, S.,
785 Weissenborn, S., Sarov, M.*, et al.* (2020). Cellular Expression and Functional Roles of All 26
786 Neurotransmitter GPCRs in the C. elegans Egg-Laying Circuit. J Neurosci *40*, 7475-7488.
787 Garcia, L.R., Mehta, P., and Sternberg, P.W. (2001). Regulation of distinct muscle behaviors controls the
788 C. elegans male's copulatory spicules during mating. Cell *107*, 777-788.
789 Gendrel, M., Atlas, E.G., and Hobert, O. (2016). A cellular and regulatory map of the GABAergic nervous
790 system of C. elegans. Elife *5*.
791 Geppetti, P., Veldhuis, N.A., Lieu, T., and Bunnett, N.W. (2015). G Protein-Coupled Receptors: Dynamic
792 Machines for Signaling Pain and Itch. Neuron *88*, 635-649.
793 Gürel, G., Gustafson, M.A., Pepper, J.S., Horvitz, H.R., and Koelle, M.R. (2012). Receptors and other
794 signaling proteins required for serotonin control of locomotion in Caenorhabditis elegans.
795 Genetics *192*, 1359-1371.
796 Hajdu-Cronin, Y.M., Chen, W.J., Patikoglou, G., Koelle, M.R., and Sternberg, P.W. (1999). Antagonism
797 between G(o)alpha and G(q)alpha in Caenorhabditis elegans: the RGS protein EAT-16 is
798 necessary for G(o)alpha signaling and regulates G(q)alpha activity. Genes Dev *13*, 1780-1793.
799 Hashimotodani, Y., Ohno-Shosaku, T., and Kano, M. (2006). [Mechanisms of triggering
800 endocannabinoid release]. Seikagaku *78*, 126-130.
801 Hashimotodani, Y., Ohno-Shosaku, T., Tanimura, A., Kita, Y., Sano, Y., Shimizu, T., Di Marzo, V., and
802 Kano, M. (2013). Acute inhibition of diacylglycerol lipase blocks endocannabinoid-mediated
803 retrograde signalling: evidence for on-demand biosynthesis of 2-arachidonoylglycerol. J Physiol
804 *591*, 4765-4776.

805 Hashimotodani, Y., Ohno-Shosaku, T., Tsubokawa, H., Ogata, H., Emoto, K., Maejima, T., Araishi, K.,
806 Shin, H.S., and Kano, M. (2005). Phospholipase Cbeta serves as a coincidence detector through
807 its Ca2+ dependency for triggering retrograde endocannabinoid signal. Neuron *45*, 257-268.
808 Hashimotodani, Y., Ohno-Shosaku, T., Watanabe, M., and Kano, M. (2007). Roles of phospholipase
809 Cbeta and NMDA receptor in activity-dependent endocannabinoid release. J Physiol *584*, 373-
810 380.
811 Hiley, E., McMullan, R., and Nurrish, S.J. (2006). The Galpha12-RGS RhoGEF-RhoA signalling pathway
812 regulates neurotransmitter release in C. elegans. Embo j *25*, 5884-5895.
813 Hoyt, J.M., Wilson, S.K., Kasa, M., Rise, J.S., Topalidou, I., and Ailion, M. (2017). The SEK-1 p38 MAP
814 Kinase Pathway Modulates Gq Signaling in Caenorhabditis elegans. G3 (Bethesda) *7*, 2979-2989.
815 Hu, S., Pawson, T., and Steven, R.M. (2011). UNC-73/trio RhoGEF-2 activity modulates Caenorhabditis
816 elegans motility through changes in neurotransmitter signaling upstream of the GSA-1/Galphas
817 pathway. Genetics *189*, 137-151.
818 Huang, K.P. (1989). The mechanism of protein kinase C activation. Trends Neurosci *12*, 425-432.
819 Hyde, R., Corkins, M.E., Somers, G.A., and Hart, A.C. (2011). PKC-1 acts with the ERK MAPK signaling
820 pathway to regulate Caenorhabditis elegans mechanosensory response. Genes Brain Behav *10*,
821 286-298.
822 Jacob, T.C., and Kaplan, J.M. (2003). The EGL-21 carboxypeptidase E facilitates acetylcholine release at
823 Caenorhabditis elegans neuromuscular junctions. J Neurosci *23*, 2122-2130.
824 Jantsch-Plunger, V., Gönczy, P., Romano, A., Schnabel, H., Hamill, D., Schnabel, R., Hyman, A.A., and
825 Glotzer, M. (2000). CYK-4: A Rho family gtpase activating protein (GAP) required for central
826 spindle formation and cytokinesis. J Cell Biol *149*, 1391-1404.

827 Jose, A.M., and Koelle, M.R. (2005). Domains, amino acid residues, and new isoforms of Caenorhabditis
828 elegans diacylglycerol kinase 1 (DGK-1) important for terminating diacylglycerol signaling in vivo.
829 J Biol Chem *280*, 2730-2736.
830 Kass, J., Jacob, T.C., Kim, P., and Kaplan, J.M. (2001). The EGL-3 proprotein convertase regulates
831 mechanosensory responses of Caenorhabditis elegans. J Neurosci *21*, 9265-9272.
832 Kim, J., Poole, D.S., Waggoner, L.E., Kempf, A., Ramirez, D.S., Treschow, P.A., and Schafer, W.R. (2001).
833 Genes affecting the activity of nicotinic receptors involved in Caenorhabditis elegans egg-laying
834 behavior. Genetics *157*, 1599-1610.
835 Konig, B., DiNitto, P.A., and Blumberg, P.M. (1985). Stoichiometric binding of diacylglycerol to the
836 phorbol ester receptor. J Cell Biochem *29*, 37-44.
837 Kopchock, R.J., 3rd, Ravi, B., Bode, A., and Collins, K.M. (2021). The sex-specific VC neurons are
838 mechanically activated motor neurons that facilitate serotonin-induced egg laying in C. elegans. J
839 Neurosci.
840 Kunitomo, H., Sato, H., Iwata, R., Satoh, Y., Ohno, H., Yamada, K., and Iino, Y. (2013). Concentration
841 memory-dependent synaptic plasticity of a taste circuit regulates salt concentration chemotaxis
842 in Caenorhabditis elegans. Nat Commun *4*, 2210.
843 Lackner, M.R., Nurrish, S.J., and Kaplan, J.M. (1999). Facilitation of synaptic transmission by EGL-30
844 Gqalpha and EGL-8 PLCbeta: DAG binding to UNC-13 is required to stimulate acetylcholine
845 release. Neuron *24*, 335-346.
846 Li, B., Jie, W., Huang, L., Wei, P., Li, S., Luo, Z., Friedman, A.K., Meredith, A.L., Han, M.H., Zhu, X.H.*, et al.*
847 (2014). Nuclear BK channels regulate gene expression via the control of nuclear calcium
848 signaling. Nat Neurosci *17*, 1055-1063.

849 Li, P., Collins, K.M., Koelle, M.R., and Shen, K. (2013). LIN-12/Notch signaling instructs postsynaptic
850 muscle arm development by regulating UNC-40/DCC and MADD-2 in Caenorhabditis elegans.
851 Elife *2*, e00378.
852 Lou, X., Korogod, N., Brose, N., and Schneggenburger, R. (2008). Phorbol esters modulate spontaneous
853 and Ca2+-evoked transmitter release via acting on both Munc13 and protein kinase C. J Neurosci
854 *28*, 8257-8267.
855 Lutz, S., Freichel-Blomquist, A., Yang, Y., Rumenapp, U., Jakobs, K.H., Schmidt, M., and Wieland, T.
856 (2005). The guanine nucleotide exchange factor p63RhoGEF, a specific link between Gq/11-
857 coupled receptor signaling and RhoA. J Biol Chem *280*, 11134-11139.
858 Maruyama, I.N., and Brenner, S. (1991). A phorbol ester/diacylglycerol-binding protein encoded by the
859 unc-13 gene of Caenorhabditis elegans. Proc Natl Acad Sci U S A *88*, 5729-5733.
860 McMullan, R., Hiley, E., Morrison, P., and Nurrish, S.J. (2006). Rho is a presynaptic activator of
861 neurotransmitter release at pre-existing synapses in C. elegans. Genes Dev *20*, 65-76.
862 McMullan, R., and Nurrish, S.J. (2011). The RHO-1 RhoGTPase modulates fertility and multiple
863 behaviors in adult C. elegans. PLoS One *6*, e17265.
864 Mendel, J.E., Korswagen, H.C., Liu, K.S., Hajdu-Cronin, Y.M., Simon, M.I., Plasterk, R.H., and Sternberg,
865 P.W. (1995). Participation of the protein Go in multiple aspects of behavior in C. elegans. Science
866 *267*, 1652-1655.
867 Miller, K.G., Alfonso, A., Nguyen, M., Crowell, J.A., Johnson, C.D., and Rand, J.B. (1996). A genetic
868 selection for Caenorhabditis elegans synaptic transmission mutants. Proc Natl Acad Sci U S A *93*,
869 12593-12598.
870 Miller, K.G., Emerson, M.D., and Rand, J.B. (1999). Goalpha and diacylglycerol kinase negatively
871 regulate the Gqalpha pathway in C. elegans. Neuron *24*, 323-333.

872 Moresco, J.J., and Koelle, M.R. (2004). Activation of EGL-47, a Galpha(o)-coupled receptor, inhibits
873 function of hermaphrodite-specific motor neurons to regulate Caenorhabditis elegans egg-laying
874 behavior. J Neurosci *24*, 8522-8530.
875 Mujica, P.E., and Gonzalez, F.G. (2011). Interaction between IP(3) receptors and BK channels in arterial
876 smooth muscle: non-canonical IP(3) signaling at work. J Gen Physiol *137*, 473-477.
877 Newton, A.C. (2001). Protein kinase C: structural and spatial regulation by phosphorylation, cofactors,
878 and macromolecular interactions. Chem Rev *101*, 2353-2364.
879 Nurrish, S., Segalat, L., and Kaplan, J.M. (1999). Serotonin inhibition of synaptic transmission: Galpha(0)
880 decreases the abundance of UNC-13 at release sites. Neuron *24*, 231-242.
881 Oakes, M., Law, W.J., and Komuniecki, R. (2019). Cannabinoids Stimulate the TRP Channel-Dependent
882 Release of Both Serotonin and Dopamine to Modulate Behavior in C. elegans. J Neurosci *39*,
883 4142-4152.
884 Oakes, M.D., Law, W.J., Clark, T., Bamber, B.A., and Komuniecki, R. (2017). Cannabinoids Activate
885 Monoaminergic Signaling to Modulate Key C. elegans Behaviors. J Neurosci *37*, 2859-2869.
886 Offermanns, S. (2001). In vivo functions of heterotrimeric G-proteins: studies in Galpha-deficient mice.
887 Oncogene *20*, 1635-1642.
888 Ohno, H., Sakai, N., Adachi, T., and Iino, Y. (2017). Dynamics of Presynaptic Diacylglycerol in a Sensory
889 Neuron Encode Differences between Past and Current Stimulus Intensity. Cell Rep *20*, 2294-
890 2303.
891 Okochi, Y., Kimura, K.D., Ohta, A., and Mori, I. (2005). Diverse regulation of sensory signaling by C.
892 elegans nPKC-epsilon/eta TTX-4. EMBO J *24*, 2127-2137.

893 Pastuhov, S.I., Matsumoto, K., and Hisamoto, N. (2016). Endocannabinoid signaling regulates
894 regenerative axon navigation in Caenorhabditis elegans via the GPCRs NPR-19 and NPR-32.
895 Genes Cells *21*, 696-705.
896 Pereira, L., Kratsios, P., Serrano-Saiz, E., Sheftel, H., Mayo, A.E., Hall, D.H., White, J.G., LeBoeuf, B.,
897 Garcia, L.R., Alon, U.*, et al.* (2015). A cellular and regulatory map of the cholinergic nervous
898 system of C. elegans. Elife *4*.
899 Porter, M.Y., and Koelle, M.R. (2010). RSBP-1 is a membrane-targeting subunit required by the
900 Galpha(q)-specific but not the Galpha(o)-specific R7 regulator of G protein signaling in
901 Caenorhabditis elegans. Mol Biol Cell *21*, 232-243.
902 Ravi, B., Garcia, J., and Collins, K.M. (2018a). Homeostatic Feedback Modulates the Development of
903 Two-State Patterned Activity in a Model Serotonin Motor Circuit in Caenorhabditis elegans. J
904 Neurosci *38*, 6283-6298.
905 Ravi, B., Nassar, L.M., Kopchock, R.J., 3rd, Dhakal, P., Scheetz, M., and Collins, K.M. (2018b).
906 Ratiometric Calcium Imaging of Individual Neurons in Behaving Caenorhabditis Elegans. J Vis Exp.
907 Ravi, B., Zhao, J., Chaudhry, I., Signorelli, R., Bartole, M., Kopchock, R.J., Guijarro, C., Kaplan, J.M., Kang,
908 L., and Collins, K.M. (2021). Presynaptic Galphao (GOA-1) signals to depress command neuron
909 excitability and allow stretch-dependent modulation of egg laying in Caenorhabditis elegans.
910 Genetics.
911 Reynolds, N.K., Schade, M.A., and Miller, K.G. (2005). Convergent, RIC-8-dependent Galpha signaling
912 pathways in the Caenorhabditis elegans synaptic signaling network. Genetics *169*, 651-670.
913 Rojas, R.J., Yohe, M.E., Gershburg, S., Kawano, T., Kozasa, T., and Sondek, J. (2007). Galphaq directly
914 activates p63RhoGEF and Trio via a conserved extension of the Dbl homology-associated
915 pleckstrin homology domain. J Biol Chem *282*, 29201-29210.

916 Rose, A.M., and Baillie, D.L. (1980). Genetic organization of the region around UNC-15 (I), a gene
917 affecting paramyosin in Caenorhabditis elegans. Genetics *96*, 639-648.
918 Rozengurt, E., Sinnett-Smith, J., and Zugaza, J.L. (1997). Protein kinase D: a novel target for
919 diacylglycerol and phorbol esters. Biochem Soc Trans *25*, 565-571.
920 Seifert, J.P., Zhou, Y., Hicks, S.N., Sondek, J., and Harden, T.K. (2008). Dual activation of phospholipase
921 C-epsilon by Rho and Ras GTPases. J Biol Chem *283*, 29690-29698.
922 Shimizu, T., Pastuhov, S.I., Hanafusa, H., Matsumoto, K., and Hisamoto, N. (2018). The C. elegans
923 BRCA2-ALP/Enigma Complex Regulates Axon Regeneration via a Rho GTPase-ROCK-MLC
924 Phosphorylation Pathway. Cell Rep *24*, 1880-1889.
925 Shyn, S.I., Kerr, R., and Schafer, W.R. (2003). Serotonin and Go modulate functional states of neurons
926 and muscles controlling C. elegans egg-laying behavior. Curr Biol *13*, 1910-1915.
927 Sieburth, D., Madison, J.M., and Kaplan, J.M. (2007). PKC-1 regulates secretion of neuropeptides. Nat
928 Neurosci *10*, 49-57.
929 Silinsky, E.M., and Searl, T.J. (2003). Phorbol esters and neurotransmitter release: more than just
930 protein kinase C? Br J Pharmacol *138*, 1191-1201.
931 Simon, M.I., Strathmann, M.P., and Gautam, N. (1991). Diversity of G proteins in signal transduction.
932 Science *252*, 802-808.
933 Soltesz, I., Alger, B.E., Kano, M., Lee, S.H., Lovinger, D.M., Ohno-Shosaku, T., and Watanabe, M. (2015).
934 Weeding out bad waves: towards selective cannabinoid circuit control in epilepsy. Nat Rev
935 Neurosci *16*, 264-277.
936 Stauffer, T.P., Ahn, S., and Meyer, T. (1998). Receptor-induced transient reduction in plasma
937 membrane PtdIns(4,5)P2 concentration monitored in living cells. Curr Biol *8*, 343-346.

938 Steven, R., Kubiseski, T.J., Zheng, H., Kulkarni, S., Mancillas, J., Ruiz Morales, A., Hogue, C.W., Pawson,
939 T., and Culotti, J. (1998). UNC-73 activates the Rac GTPase and is required for cell and growth
940 cone migrations in C. elegans. Cell *92*, 785-795.
941 Steven, R., Zhang, L., Culotti, J., and Pawson, T. (2005). The UNC-73/Trio RhoGEF-2 domain is required
942 in separate isoforms for the regulation of pharynx pumping and normal neurotransmission in C.
943 elegans. Genes Dev *19*, 2016-2029.
944 Tabuse, Y. (2002). Protein kinase C isotypes in C. elegans. J Biochem *132*, 519-522.
945 Tabuse, Y., Nishiwaki, K., and Miwa, J. (1989). Mutations in a protein kinase C homolog confer phorbol
946 ester resistance on Caenorhabditis elegans. Science *243*, 1713-1716.
947 Tanimura, A., Yamazaki, M., Hashimotodani, Y., Uchigashima, M., Kawata, S., Abe, M., Kita, Y.,
948 Hashimoto, K., Shimizu, T., Watanabe, M.*, et al.* (2010). The endocannabinoid 2-
949 arachidonoylglycerol produced by diacylglycerol lipase alpha mediates retrograde suppression of
950 synaptic transmission. Neuron *65*, 320-327.
951 Tanis, J.E., Moresco, J.J., Lindquist, R.A., and Koelle, M.R. (2008). Regulation of serotonin biosynthesis
952 by the G proteins Galphao and Galphaq controls serotonin signaling in Caenorhabditis elegans.
953 Genetics *178*, 157-169.
954 Tewson, P., Westenberg, M., Zhao, Y., Campbell, R.E., Quinn, A.M., and Hughes, T.E. (2012).
955 Simultaneous detection of Ca2+ and diacylglycerol signaling in living cells. PLoS One *7*, e42791.
956 Thomas, J.H. (1990). Genetic analysis of defecation in Caenorhabditis elegans. Genetics *124*, 855-872.
957 Thore, S., Dyachok, O., Gylfe, E., and Tengholm, A. (2005). Feedback activation of phospholipase C via
958 intracellular mobilization and store-operated influx of Ca2+ in insulin-secreting beta-cells. J Cell
959 Sci *118*, 4463-4471.

960 Trent, C., Tsuing, N., and Horvitz, H.R. (1983). Egg-laying defective mutants of the nematode
961 Caenorhabditis elegans. Genetics *104*, 619-647.
962 Vázquez-Manrique, R.P., Nagy, A.I., Legg, J.C., Bales, O.A., Ly, S., and Baylis, H.A. (2008). Phospholipase
963 C-epsilon regulates epidermal morphogenesis in Caenorhabditis elegans. PLoS Genet *4*,
964 e1000043.
965 Waggoner, L.E., Dickinson, K.A., Poole, D.S., Tabuse, Y., Miwa, J., and Schafer, W.R. (2000). Long-term
966 nicotine adaptation in Caenorhabditis elegans involves PKC-dependent changes in nicotinic
967 receptor abundance. J Neurosci *20*, 8802-8811.
968 Waggoner, L.E., Zhou, G.T., Schafer, R.W., and Schafer, W.R. (1998). Control of alternative behavioral
969 states by serotonin in Caenorhabditis elegans. Neuron *21*, 203-214.
970 Wettschureck, N., van der Stelt, M., Tsubokawa, H., Krestel, H., Moers, A., Petrosino, S., Schütz, G., Di
971 Marzo, V., and Offermanns, S. (2006). Forebrain-specific inactivation of Gq/G11 family G
972 proteins results in age-dependent epilepsy and impaired endocannabinoid formation. Mol Cell
973 Biol *26*, 5888-5894.
974 White, J.G., Southgate, E., Thomson, J.N., and Brenner, S. (1986). The structure of the nervous system
975 of the nematode Caenorhabditis elegans. Philos Trans R Soc Lond B Biol Sci *314*, 1-340.
976 Wilkie, T.M., Gilbert, D.J., Olsen, A.S., Chen, X.N., Amatruda, T.T., Korenberg, J.R., Trask, B.J., de Jong,
977 P., Reed, R.R., Simon, M.I.*, et al.* (1992). Evolution of the mammalian G protein alpha subunit
978 multigene family. Nat Genet *1*, 85-91.
979 Williams, S.L., Lutz, S., Charlie, N.K., Vettel, C., Ailion, M., Coco, C., Tesmer, J.J., Jorgensen, E.M.,
980 Wieland, T., and Miller, K.G. (2007). Trio's Rho-specific GEF domain is the missing Galpha q
981 effector in C. elegans. Genes Dev *21*, 2731-2746.

982 Wing, M.R., Snyder, J.T., Sondek, J., and Harden, T.K. (2003). Direct activation of phospholipase C-
983 epsilon by Rho. J Biol Chem *278*, 41253-41258.
984 Xiao, H., Hapiak, V.M., Smith, K.A., Lin, L., Hobson, R.J., Plenefisch, J., and Komuniecki, R. (2006). SER-1,
985 a Caenorhabditis elegans 5-HT2-like receptor, and a multi-PDZ domain containing protein (MPZ-
986 1) interact in vulval muscle to facilitate serotonin-stimulated egg-laying. Dev Biol *298*, 379-391.
987 Xiao, L., Eto, M., and Kazanietz, M.G. (2009). ROCK mediates phorbol ester-induced apoptosis in
988 prostate cancer cells via p21Cip1 up-regulation and JNK. J Biol Chem *284*, 29365-29375.
989 Yang, L., Dai, F., Tang, L., Le, Y., and Yao, W. (2017). Macrophage differentiation induced by PMA is
990 mediated by activation of RhoA/ROCK signaling. J Toxicol Sci *42*, 763-771.
991 Yin, X., Gower, N.J., Baylis, H.A., and Strange, K. (2004). Inositol 1,4,5-trisphosphate signaling regulates
992 rhythmic contractile activity of myoepithelial sheath cells in Caenorhabditis elegans. Mol Biol
993 Cell *15*, 3938-3949.
994 Yu, H., Aleman-Meza, B., Gharib, S., Labocha, M.K., Cronin, C.J., Sternberg, P.W., and Zhong, W. (2013).
995 Systematic profiling of Caenorhabditis elegans locomotive behaviors reveals additional
996 components in G-protein Galphaq signaling. Proc Natl Acad Sci U S A *110*, 11940-11945.
997 Zhang, M., Chung, S.H., Fang-Yen, C., Craig, C., Kerr, R.A., Suzuki, H., Samuel, A.D., Mazur, E., and
998 Schafer, W.R. (2008). A self-regulating feed-forward circuit controlling C. elegans egg-laying
999 behavior. Curr Biol *18*, 1445-1455.
1000 Zhang, M., Schafer, W.R., and Breitling, R. (2010). A circuit model of the temporal pattern generator of
1001 Caenorhabditis egg-laying behavior. BMC Syst Biol *4*, 81.
1002